Testing Conditional Independence in Supervised Learning Algorithms

David S. Watson*

Oxford Internet Institute, University of Oxford, Oxford, UK

Queen Mary University of London, London, UK

and

Marvin N. Wright

Leibniz Institute for Prevention Research and Epidemiology – BIPS, Bremen, Germany

December 17, 2019

Abstract

We propose the conditional predictive impact (CPI), a consistent and unbiased estimator of the association between one or several features and a given outcome, conditional on a reduced feature set. Building on the knockoff framework of Candès et al. (2018), we develop a novel testing procedure that works in conjunction with any valid knockoff sampler, supervised learning algorithm, and loss function. The CPI can be efficiently computed for high-dimensional data without any sparsity constraints. We demonstrate convergence criteria for the CPI and develop statistical inference procedures for evaluating its magnitude, significance, and precision. These tests aid in feature and model selection, extending traditional frequentist and Bayesian techniques to general supervised learning tasks. The CPI may also be applied in causal discovery to identify underlying multivariate graph structures. We test our method using various algorithms, including linear regression, neural networks, random forests, and support vector machines. Empirical results show that the CPI compares favorably to alternative variable importance measures and other nonparametric tests of conditional independence on a diverse array of real and simulated datasets. Simulations confirm that our inference procedures successfully control Type I error and achieve nominal coverage probability. Our method has been implemented in an R package, `cpi`, which can be downloaded from https://github.com/dswatson/cpi.

Keywords: Knockoffs, machine learning, Markov blanket, variable importance.

---

*david.watson@oii.ox.ac.uk

1   Introduction

Variable importance (VI) is a major topic in statistics and machine learning. It is the basis of most if not all feature selection methods, which analysts use to identify key drivers of variation in an outcome of interest and/or create more parsimonious models (Guyon and Elisseeff, 2003; Kuhn and Johnson, 2019; Meinshausen and Bühlmann, 2010). Many importance measures have been proposed in recent years, either for specific algorithms or more general applications. Several different notions of VI – some overlapping, some inconsistent – have emerged from this literature. We examine these in greater detail in Section 2.1.

One fundamental difference between various importance measures is whether they test the marginal or conditional independence of features. To evaluate response variable Y's marginal dependence on predictor X_j, we test against the following hypothesis:

$$\text{Marginal:}$$
$$H_0 : X_j \perp\!\!\!\perp Y, \mathbf{X}_{-j}$$

where $\mathbf{X}_{-j}$ denotes a set of covariates. A measure of conditional dependence, on the other hand, tests against a different null hypothesis:

$$\text{Conditional:}$$
$$H_0 : X_j \perp\!\!\!\perp Y | \mathbf{X}_{-j}$$

Note that X_j's marginal VI may be high due to its association with either Y or $\mathbf{X}_{-j}$. This is why measures of marginal importance tend to favor correlated predictors. Often, however, our goal is to determine whether X_j adds any *new* information – in other words, whether Y is dependent on X_j even after conditioning on $\mathbf{X}_{-j}$. This becomes especially important when the assumption of feature independence is violated.

Tests of conditional independence (CI) are common in the causal modelling literature. For instance, the popular PC algorithm (Spirtes et al., 2000), which infers a set of underlying directed acyclic graphs (DAGs) consistent with some observational data, relies on the results of CI tests to recursively remove the edges between nodes. Common parametric examples include the partial correlation test for continuous variables or the χ^2 test

for categorical data. A growing body of literature in recent years has examined nonparametric alternatives to these options. We provide an overview of several such proposals in Section 2.2.

In this paper, we introduce a new CI test to measure VI. The conditional predictive impact (CPI) quantifies the contribution of one or several features to a given algorithm's predictive performance, conditional on a complementary feature subset. Our work relies on so-called "knockoff" variables (formally defined in Section 2.3) to provide negative controls for feature testing. Because knockoffs are, by construction, exchangeable with their observed counterparts and conditionally independent of the response, they enable a paired testing approach without any model refitting. Unlike the original knockoff filter, however, our methods are not limited to certain types of datasets or algorithms.

The CPI is extremely general. It can be used with any combination of knockoff sampler, supervised learner, and loss function. It can be efficiently computed in low or high dimensions without sparsity constraints. We demonstrate that the CPI is an unbiased estimator, provably consistent under minimal assumptions. We develop statistical inference procedures for evaluating its magnitude, precision, and significance. Finally, we demonstrate the measure's utility on a variety of real and simulated datasets.

The remainder of this paper is structured as follows. We review related work in Section 2. We present theoretical results in Section 3, where we also outline an efficient algorithm for estimating the CPI, along with corresponding p-values and confidence intervals. We test our procedure on real and simulated data in Section 4, comparing its performance with popular alternatives under a variety of regression and classification settings. Following a discussion in Section 5, we conclude in Section 6.

2   Related Work

In this section, we survey the relevant literature on VI estimation, CI tests, and the knockoff filter.

2.1 Variable Importance Measures

The notion of VI may feel fairly intuitive at first, but closer inspection reveals a number of underlying ambiguities. One important dichotomy is that between global and local measures, which respectively quantify the impact of features on all or particular predictions. This distinction has become especially important with the recent emergence of interpretable machine learning techniques designed to explain individual outputs of black box models (e.g., Datta et al., 2016; Lundberg and Lee, 2017; Ribeiro et al., 2016; Wachter et al., 2018). In what follows, we restrict our focus to global importance measures.

Another important dichotomy is that between model-specific and model-agnostic approaches. For instance, a number of methods have been proposed for estimating importance in linear regression (Barber and Candès, 2015; Grömping, 2007; Lindeman et al., 1980), random forests (Breiman, 2001; Kursa and Rudnicki, 2010; Strobl et al., 2008), and neural networks (Bach et al., 2015; Gevrey et al., 2003; Shrikumar et al., 2017). These measures have the luxury of leveraging an algorithm's underlying assumptions and internal architecture for more precise and efficient VI estimation.

Other, more general techniques have also been developed. Van der Laan (2006) derives efficient influence curves and inference procedures for a variety of VI measures. Hubbard et al. (2018) build on this work, proposing a data-adaptive method for estimating the causal influence of variables within the targeted maximum likelihood framework (van der Laan and Rose, 2018). Williamson et al. (2017) describe an ANOVA-style decomposition of a regressor's R^2 into feature-wise contributions. Feng et al. (2018) design a neural network to efficiently compute this decomposition using multi-task learning. Fisher et al. (2018) propose a number of "reliance" statistics, calculated by integrating a loss function over the empirical distribution of covariates while holding a given feature vector constant.

Perhaps the most important distinction between various competing notions of VI is the aforementioned split between marginal and conditional measures. The topic has received considerable attention in the random forest literature, where Breiman's popular permutation technique (2001) has been criticized for failing to properly account for correlations between features (Gregorutti et al., 2015; Nicodemus et al., 2010). Conditional alternatives

have been developed (Mentch and Hooker, 2016; Strobl et al., 2008), but we do not consider them here, as they are specific to tree ensembles.

Our proposed measure resembles what Fisher et al. (2018) call "algorithm reliance" (AR). The authors do not have much to say about AR in their paper, the majority of which is instead devoted to two related statistics they term "model reliance" (MR) and "model class reliance" (MCR). These measure the marginal importance of a feature subset in particular models or groups of models, respectively. Only AR measures the importance of the subset conditional on remaining covariates for a given supervised learner, which is our focus here. Fisher et al. derive probabilistic bounds for MR and MCR, but not AR. They do not develop hypothesis testing procedures for any of their reliance statistics.

2.2 Conditional Independence Tests

CI tests are the cornerstone of constraint-based and hybrid methods for causal graph inference and Bayesian network learning (Koller and Friedman, 2009; Korb and Nicholson, 2009; Scutari and Denis, 2014). Assuming the causal Markov condition and faithfulness – which together state (roughly) that statistical independence implies graphical independence and vice versa – a number of algorithms have been developed that use CI tests to discover an equivalence class of DAGs consistent with a set of observational data (Maathuis et al., 2009; Verma and Pearl, 1991; Spirtes et al., 2000).

Shah and Peters (forthcoming) have shown that there exists no uniformly valid CI test. Parametric assumptions are typically deployed to restrict the range of alternative hypotheses, which is default behavior for most causal discovery software (e.g., Kalisch et al., 2012; Scutari, 2010). However, more flexible methods have been introduced. Much of this literature relies on techniques that embed the data in a reproducing kernel Hilbert space (RKHS). For instance, Fukumizu et al. (2008) use a normalized cross-covariance operator to test the association between features in the RKHS. A null distribution is approximated via permutation. Doran et al. (2014) build on Fukumizu et al.'s work with a modified permutation scheme intended to capture the effects of CI. Zhang et al. (2011) derive a test statistic from the traces of kernel matrices, using a gamma null distribution to compute

statistical significance.

Because kernel methods do not scale well with sample size, several authors have proposed more efficient alternatives. For instance, Strobl et al. (2018) employ a fast Fourier transform to reduce the complexity of matrix operations. Methods have been developed for estimating regularized, nonlinear partial correlations (Ramsey, 2014; Shah and Peters, forthcoming). Lei et al. (2018) and Rinaldo et al. (2019) study the leave-one-covariate-out (LOCO) procedure, in which an algorithm is trained on data with and without the variable of interest. The predictive performance of nested models is compared to evaluate the conditional importance of the dropped feature.

Our proposal is conceptually similar to LOCO, which can in principle be extended to feature subsets of arbitrary dimension. The method enjoys some especially nice statistical properties when used in conjunction with sample splitting. For instance, Rinaldo et al. derive a central limit theorem for LOCO parameters, while Lei et al. prove finite sample error control using conformal inference. However, retraining an algorithm for each CI test is potentially infeasible, especially for complex learners and/or large datasets. With knockoffs, we can directly import LOCO's statistical guarantees without any model refitting.

2.3   The Knockoff Framework

Our work builds on the knockoff procedure originally conceived by Barber and Candès (2015) and later refined by Candès et al. (2018). Central to this approach is the notion of a *knockoff variable*. Given an $n \times p$ input matrix $\mathbf{X}$, we define a knockoff matrix of equal dimensionality $\tilde{\mathbf{X}}$ as any matrix that meets the following two criteria:

(a) **Pairwise exchangeability.** For any proper subset $S \subset [p] = (1, \ldots, p)$:

$$(\mathbf{X}, \tilde{\mathbf{X}})_{swap(S)} \overset{d}{=} (\mathbf{X}, \tilde{\mathbf{X}})$$

where $\overset{d}{=}$ represents equality in distribution and the swapping operation is defined below.

(b) **Conditional independence**. $\tilde{\mathbf{X}} \perp\!\!\!\perp Y | \mathbf{X}$.

A swap is obtained by switching the entries X_j and $\tilde{X}_j$ for each $j \in S$. For example, with $p = 3$ and $S = \{1, 3\}$:

$$(X_1, X_2, X_3, \tilde{X}_1, \tilde{X}_2, \tilde{X}_3)_{swap(S)} \overset{d}{=} (\tilde{X}_1, X_2, \tilde{X}_3, X_1, \tilde{X}_2, X_3)$$

Knockoffs provide negative controls for conditional independence testing. The intuition behind the method is that if X_j does not significantly outperform $\tilde{X}_j$ by some relevant importance measure, then the original feature may be safely removed from the final model.

Practical implementation requires both a method for generating knockoffs and a decision procedure for variable selection. The subject has quickly become a busy one in statistics and machine learning, with most authors focusing on the former task. In this paper, we instead tackle the latter, developing a general framework for testing conditional VI.

Constructing nontrivial knockoffs is a considerable challenge. Numerous methods have been proposed, including but not limited to:

- Second-order Gaussian knockoffs (Candès et al., 2018)
- Conditional permutation sampling (Berrett et al., 2019)
- Hidden Markov model sampling (Sesia et al., 2018)
- Conditional density estimation (Tansey et al., 2018)
- Generative deep neural networks (Romano et al., 2018; Jordon et al., 2019)
- Metropolis-Hastings sampling (Bates et al., 2019)

A complete review of these proposals is beyond the scope of this paper. Bates et al. (2019) demonstrate that no efficient knockoff sampler exists for arbitrary probability distributions, suggesting that algorithms will have to make some assumptions about the data generating process to strike a reasonable balance between sensitivity and specificity.

The original knockoff papers introduce a novel algorithm for controlling the false discovery rate (FDR) in variable selection problems. The goal is to find the minimal subset $\mathcal{S} \subset [p]$ such that, conditional on $\{X_j\}_{j \in \mathcal{S}}$, Y is independent of all other variables. Call this the Markov blanket of Y (Pearl, 1988). Null features form a complementary set $\mathcal{R} = [p] \setminus \mathcal{S}$ such that $k \in \mathcal{R}$ if and only if $X_k \perp\!\!\!\perp Y | \{X_j\}_{j \in \mathcal{S}}$. The FDR is given by the expected

proportion of false positives among all declared positives:

$$\text{FDR} = \mathbb{E}\left[\frac{|\widehat{\mathcal{S}} \cap \mathcal{R}|}{|\widehat{\mathcal{S}}| \vee 1}\right]$$

where $\widehat{\mathcal{S}}$ is the output of the decision procedure and the "$\vee$ 1" in the denominator enforces the convention that $\text{FDR} = 0$ when $|\widehat{\mathcal{S}}| = 0$.

Barber and Candès (2015) demonstrate a method for guaranteed finite sample FDR control when (i) statistics for null variables are symmetric about zero and (ii) large positive statistics indicate strong evidence against the null. We will henceforth refer to this method as the adaptive thresholding test (ATT). Unlike other common techniques for controlling the FDR (e.g., Benjamini and Hochberg, 1995; Benjamini and Yekutieli, 2001; Storey, 2002), the ATT does not require p-values as an intermediate step. Candès et al. (2018) argue that this is a benefit in high-dimensional settings, where p-value calculations can be unreliable.

Acknowledging that p-values may still be desired in some applications, however, Candès et al. also propose the conditional randomization test (CRT), which provides one-sided Monte Carlo p-values by repeatedly sampling from the knockoff distribution. Experiments indicate that the CRT is slightly more powerful than the ATT, but the authors caution that the former is very computationally intensive and do not recommend it for large datasets. That has not stopped other groups from advancing formally similar proposals (e.g., Berrett et al., 2019; Tansey et al., 2018).

We highlight several important shortcomings of the ATT:

1. Not all algorithms provide feature scoring statistics.

2. The ATT requires a large number of variables to reliably detect true positives.

3. Because the ATT does not perform individual hypothesis tests, it cannot provide confidence or credible intervals for particular variables.

In what follows, we present alternative inference procedures for conditional independence testing designed to address all three issues.

3   Conditional Predictive Impact

The basic intuition behind our approach is that important features should be *informative* — that is, their inclusion should improve the predictive performance of an appropriate algorithm as measured by some preselected loss function. Moreover, the significance of improvement should be quantifiable so that error rates can be controlled at user-specified levels.

Consider an $n \times p$ feature matrix $\mathbf{X} \in \mathcal{X}$ and corresponding $n \times 1$ response variable $Y \in \mathcal{Y}$, which combine to form the dataset $\mathbf{Z} = (\mathbf{X}, Y) \in \mathcal{Z}$. Each observation $\mathbf{z}_i = (\mathbf{x}_i, y_i)$ is an i.i.d. sample from a fixed but unknown joint probability distribution, $\mathbb{P}(\mathbf{Z}) = \mathbb{P}(\mathbf{X}, Y)$. Let $\mathbf{X}^S \subseteq (X_1, \ldots, X_p)$ denote some subset of the feature space whose predictive impact we intend to quantify, conditional on the (possibly empty) set of remaining covariates $\mathbf{X}^R = \mathbf{X} \setminus \mathbf{X}^S$. Data can now be expressed as a triple, $\mathbf{Z} = (\mathbf{X}^S, \mathbf{X}^R, Y)$. We remove the predictive information in $\mathbf{X}^S$ while preserving the covariance structure of the predictors by replacing the submatrix with the corresponding knockoff variables, $\tilde{\mathbf{X}}^S$, rendering a new dataset, $\tilde{\mathbf{Z}} = (\tilde{\mathbf{X}}^S, \mathbf{X}^R, Y)$.

Define a function $f \in \mathcal{F}, \mathcal{F} : \mathcal{X} \to \mathcal{Y}$ as a mapping from features to outcomes. We evaluate a model's performance using some real-valued, nonnegative loss function $L : \mathcal{F} \times \mathcal{Z} \to \mathbb{R}_{\geq 0}$. Define the risk of f with respect to $\mathbf{Z}$ as its expected loss over the joint probability distribution $\mathbb{P}(\mathbf{Z})$:

$$R(f, \mathbf{Z}) = \mathbb{E}[L(f, \mathbf{Z})]$$

Our strategy is to replace the conditional null hypothesis defined in Section 1 with the following:

<div align="center">

Conditional Predictive:

$$H_0 : R(f, \mathbf{Z}) \geq R(f, \tilde{\mathbf{Z}})$$

</div>

In other words, we test whether the model performs better using the original or the knockoff data.

3.1 Consistency and Convergence

The CPI of submatrix $\mathbf{X}^S$ measures the extent to which the feature subset improves predictions made using model f. Assume that the loss function L can be evaluated for each sample i.[1] We define the following random variable:

$$\Delta_i = L(f, \tilde{\mathbf{z}}_i) - L(f, \mathbf{z}_i) \tag{1}$$

This vector represents the difference in sample-wise loss between predictions made using knockoff data and original data. We define the CPI by taking its expectation:

$$\text{CPI}(\mathbf{X}^S) = \mathbb{E}[\Delta] \tag{2}$$

Note that the CPI is always a function of some feature subset $\mathbf{X}^S$. We suppress the dependency for notational convenience moving forward.

To consistently estimate this statistic, it is necessary and sufficient to show that we can consistently estimate the risk of model f. The population parameter $R(f, \mathbf{Z})$ is estimated using the empirical risk formula:

$$R_{\text{emp}}(f, \mathbf{Z}) = \frac{1}{m} \sum_{i=1}^{m} L(f, \mathbf{z}_i) \tag{3}$$

Our goal in estimating risk is to evaluate how well the model generalizes beyond its training data, so the m samples in Eq. 3 constitute a test set drawn independently from $\mathbf{Z}$, distinct from the n samples used to fit f. In practice, this is typically achieved by some resampling procedure like cross-validation or bootstrapping. In what follows, we presume that unit-level loss $L(f, \mathbf{z}_i)$ is always an out-of-sample evaluation, such that f was trained on data excluding $\mathbf{z}_i$.

The empirical risk minimization (ERM) principle is a simple decision procedure in which we select the function f that minimizes empirical risk in some function space $\mathcal{F}$. A celebrated result of Vapnik and Chervonenkis (1971), independently derived by Sauer (1972) and Shelah (1972), is that the ERM principle is consistent with respect to $\mathcal{F}$ if and

---

[1]For loss functions that do not have this property, such as the area under the receiver operating characteristic curve, the following arguments can easily be modified to apply to each fold in a cross-validation.

only if the function space is of finite VC dimension. Thus, for any algorithm that meets this minimal criterion, the empirical risk $R_{\text{emp}}(f, \mathbf{Z})$ converges uniformly in probability to $R(f, \mathbf{Z})$ as $n \to \infty$, which means the estimate

$$
\begin{aligned}
\widehat{\text{CPI}} &= \frac{1}{n} \sum_{i=1}^{n} L(f, \tilde{\mathbf{z}}_i) - L(f, \mathbf{z}_i) \\
&= R_{\text{emp}}(f, \tilde{\mathbf{Z}}) - R_{\text{emp}}(f, \mathbf{Z}) \\
&= \frac{1}{n} \sum_{i=1}^{n} \Delta_i
\end{aligned}
\tag{4}
$$

is likewise guaranteed to converge.

Inference procedures for the CPI can be designed using any paired difference test. Familiar frequentist examples include the t-test and the Fisher exact test, which we use for large- and small-sample settings, respectively. Bayesian analogues can easily be implemented as well. Rouder et al. (2009) advocate an analytic strategy for calculating Bayes factors for t-tests. Wetzels et al. (2009) and Kruschke (2013) propose more general methods based on Markov chain Monte Carlo sampling, although they differ in their proposed priors and decision procedures. Care should be taken when selecting a prior distribution in the Bayesian setting, especially with small sample sizes. Tools for Bayesian inference are implemented in the `cpi` package; however, for brevity's sake, we restrict the following sections to frequentist methods.

3.2 Large Sample Inference: Paired t-tests

By the central limit theorem, empirical risk estimates for functions of finite VC dimension will tend to be normally distributed around the true population parameter value. We therefore use paired, one-sided t-tests to evaluate statistical significance when samples are sufficiently large.

The variable Δ has mean $\widehat{\text{CPI}}$ and standard error $\text{SE} = s/\sqrt{n}$, where

$$
s = \sqrt{\frac{1}{n-1} \sum_{i=1}^{n} (\Delta_i - \widehat{\text{CPI}})^2}.
$$

The t-score for $\widehat{\text{CPI}}$ is given by $t = \widehat{\text{CPI}}/\text{SE}$, and we compute p-values by comparing this statistic to the most tolerant distribution consistent with $H_0 : R(f, \mathbf{Z}) \geq R(f, \tilde{\mathbf{Z}})$, namely t_{n-1}. To control Type I error at level α, we reject H_0 for all t greater than or equal to the $(1 - \alpha)$ quantile of t_{n-1}. This procedure can easily be modified to adjust for multiple testing.

We can relax the assumption of homoskedasticity if reliable estimates of predictive precision are available. Construct a $2n \times (n + 1)$ feature matrix $\mathbf{X}$ with columns for each unit $i = \{1, \ldots, n\}$, as well as an indicator variable for data type D (original vs. knockoff). Let $\mathbf{W}$ be a $2n \times 2n$ diagonal matrix such that $\mathbf{W}_{ii}$ denotes the weight assigned to the ith prediction. For instance, in a regression setting, this could be the inverse of the expected residual variance for i. Then solve a weighted least squares regression, with the response variable $\mathbf{y}$ equal to the observed loss for each unit-data type combination:

$$\hat{\gamma} = (\mathbf{X}^\top \mathbf{W} \mathbf{X})^{-1} \mathbf{X}^\top \mathbf{W} \mathbf{y}$$

The t-statistic and p-value associated with coefficient $\hat{\gamma}_D$ can then be used to test the CPI of the substituted variable(s) under a heteroskedastic error model.

Confidence intervals around $\widehat{\text{CPI}}$ may be constructed in the typical manner. The lower bound is set by subtracting from our point estimate the product of SE and $F_{n-1}^{-1}(1 - \alpha)$, where $F_{n-1}(\cdot)$ denotes the CDF of t_{n-1}. Using this formula, we obtain a 95% confidence interval for $\widehat{\text{CPI}}$ by calculating $[\widehat{\text{CPI}} - \text{SE} \times F_{n-1}^{-1}(0.95), \infty)$. As n grows large, this interval converges to the Wald-type interval, $[\widehat{\text{CPI}} - \text{SE} \times \Phi^{-1}(0.95), \infty)$, where Φ represents the standard normal CDF.

The t-testing framework also allows for analytic power calculations. Let t^* denote the critical value $t^* = F_{n-1}^{-1}(1 - \alpha)$. Then Type II error is given by the formula $\beta = F_{n-1}(t^* - \delta)$, where δ represents the postulated effect size. Statistical power is just the complement $1 - \beta$, and rearranging this equation with simple algebra allows us to determine the sample size required to detect a given effect at some fixed Type I error α.

3.3 Small Sample Inference: Fisher Exact Tests

The applicability of the central limit theorem is dubious when sample sizes are small. In such cases, exact p-values may be computed for a slightly modified null hypothesis using Fisher's method (1935). Rather than focusing on overall risk, this null hypothesis states that replacing $\mathbf{X}^S$ with the knockoff submatrix $\tilde{\mathbf{X}}^S$ has no impact on unit-level loss. More formally, we test against the following:

$$H_0^{\text{FEP}} : L(f, \mathbf{z}_i) \geq L(f, \tilde{\mathbf{z}}_i), \quad i = 1, \ldots, n.$$

Under this null hypothesis, which is sufficient but unnecessary for the conditional predictive H_0, we may implement a permutation scheme in which the CPI is calculated for all possible assignments of data type D. Consider a $2n \times 3$ matrix with columns for unit index $U = \{1, 1, \ldots, n, n\}$, data type $D \in \{0, 1\}$, and loss L. We permute the rows of D subject to the constraint that every sample's loss is recorded under both original and knockoff predictions. For each possible vector D, compute the resulting CPI and compare the value of our observed statistic, $\widehat{\text{CPI}}$, to the complete distribution. Note that this paired setup dramatically diminishes the possible assignment space from an unmanageable $\binom{2n}{n}$, corresponding to a Bernoulli trial design, to a more reasonable 2^n. The one-tailed Fisher exact p-value (FEP) is given by the formula:

$$\text{FEP}(\widehat{\text{CPI}}) = \frac{1}{2^n} \sum_{b=1}^{2^n} \mathbb{1}(\widetilde{\text{CPI}}_b \geq \widehat{\text{CPI}})$$

where $\mathbb{1}(\cdot)$ represents the indicator function and $\widetilde{\text{CPI}}_b$ is the CPI resulting from the bth permutation of D.

To construct a confidence interval for $\widehat{\text{CPI}}$ at level $1 - \alpha$, we use our empirical null distribution. Find the critical value CPI^* such that $\text{FEP}(\text{CPI}^*) = \alpha$. Then a $(1 - \alpha) \times 100\%$ confidence interval for $\widehat{\text{CPI}}$ is given by $[\widehat{\text{CPI}} - \text{CPI}^*, \infty)$. For n large, approximate calculations can be made by sampling from the set of 2^n permissible permutations. In this case, however, it is important to add 1 to both the numerator and denominator to ensure unbiased inference (Phipson and Smyth, 2010).

3.4 Computational Complexity

To summarize, we outline our proposed algorithm for testing the conditional importance of feature subsets for supervised learners in pseudocode below.

Algorithm 1: CPI Algorithm

Input: Dataset $\mathbf{Z}$, submatrix $\mathbf{X}^S$, supervised learner a, risk functional R, knockoff sampler g, risk estimator k, inference procedure h

1. Train a on $\mathbf{Z}$ to create f

2. Apply g to generate the knockoff matrix $\tilde{\mathbf{X}}^S$

3. Use risk estimator k to compute each $L(f, \mathbf{z}_i)$ and $L(f, \tilde{\mathbf{z}}_i)$

4. Compute $\widehat{\mathrm{CPI}} = n^{-1} \sum_{i=1}^{n} L(f, \tilde{\mathbf{z}}_i) - L(f, \mathbf{z}_i)$

5. Apply inference procedure h to determine associated p-value (p) and confidence interval (ci)

Output: $\widehat{\mathrm{CPI}}$, p, ci

This algorithm executes in $\mathcal{O}(ak + g + h)$ time. We take the complexity of the learner a and knockoff sampler g to be given. The empirical risk estimator k can be made more or less complex depending on the resampling procedure. The most efficient option for evaluating generalization error is the holdout method, in which a model is trained on a random subset of the available data and tested on the remainder. Unfortunately, this procedure can be unreliable with small sample sizes. Popular alternatives include the bootstrap and cross-validation. Both require considerable model refitting, which can be costly when a is complex.

The inference procedure h is quite efficient in the parametric case – on the order of $\mathcal{O}(n)$ for the t-test – but scales exponentially with the sample size when using the permutation-based approach. As noted above, the complexity of the Fisher test can be bounded by setting an upper limit on the number of permutations B used to approximate the empirical null distribution. The standard error of a p-value estimate made using such an approxima-tion is $\sqrt{p^*(1 - p^*)/B}$, where p^* represents the true p-value. This expression is maximized

at $p^* = 0.5$, corresponding to a standard error of $1/(2\sqrt{B})$. Thus, to guarantee a standard error of at most 0.001, it would suffice to use $B = 250,000$ permutations, an eminently feasible computation using parallel processors.

4 Experiments

All experiments were conducted in the R statistical computing environment, version 3.5.1. Code for reproducing all results and figures can be found in our dedicated GitHub repository: https://github.com/dswatson/cpi_paper.

4.1 Simulated Data

We report results from a number of simulation studies. First, we analyze the statistical properties of our proposed tests under null and alternative hypotheses. We proceed to compare the sensitivity and specificity of the CPI to those of several alternative measures.

Data were simulated under four scenarios, corresponding to all combinations of independent vs. correlated predictors and linear vs. nonlinear outcomes. Because conditional importance is most relevant in the case of correlated predictors, results for the two scenarios with independent features are left to the supplement. In the linear setting, ten variables were drawn from a multivariate Gaussian distribution $\mathcal{N}(0, \Sigma)$, with covariance matrix $\Sigma_{ij} = 0.5^{|i-j|}$. A continuous outcome Y was calculated as $Y = \mathbf{X}\boldsymbol{\beta} + \epsilon$, where $\boldsymbol{\beta} = (0.0, 0.1, \ldots, 0.9)^\top$ and $\epsilon \sim \mathcal{N}(0, 1)$. In the nonlinear scenario, we keep the same predictors but generate the response from a transformed matrix, $Y = \mathbf{X}^*\boldsymbol{\beta} + \epsilon$, where

$$
x_{ij}^* = \begin{cases} +1, & \text{if } \Phi^{-1}(0.25) \leq x_{ij} \leq \Phi^{-1}(0.75) \\ -1, & \text{else} \end{cases}
$$

with the same $\boldsymbol{\beta}$ and ϵ as in the linear case. A similar simulation was performed for a classification outcome, where the response Y was drawn from a binomial distribution with probability $[1+\exp(-\mathbf{X}\boldsymbol{\beta})]^{-1}$ and $[1+\exp(-\mathbf{X}^*\boldsymbol{\beta})]^{-1}$ for the linear and nonlinear scenarios, respectively.

15

Knockoffs for all simulated data were generated using the second-order Gaussian technique described in (Candès et al., 2018) and implemented in the `knockoff` package, version 0.3.2 (Patterson and Sesia, 2018).

4.1.1 Type I and Type II Errors

We simulate $10,000$ datasets with $n = 1,000$ observations and compute the CPI using four different learning algorithms: linear/logistic regression (LM), random forests (RF), artificial neural network (ANN), and support vector machine (SVM). Risk was estimated using holdout sampling with a train/test ratio of 2:1. For regression models, we used mean square error (MSE) and mean absolute error (MAE) loss functions; for classification, we used cross entropy (CE) and mean misclassification error (MMCE). We computed p-values via the inference procedures described in Section 3, i.e. paired t-tests and Fisher exact tests. For Fisher tests we used $10,000$ permutations.

Linear and logistic regressions were built using the functions `lm()` and `glm()`, respectively, from the R package `stats` (R Core Team, 2018). RFs were built using the `ranger` package (Wright and Ziegler, 2017), with 500 trees. ANNs were built with the `nnet` package (Venables and Ripley, 2002), with 20 hidden units and a weight decay of 0.1. SVMs were built with the `e1071` package (Meyer et al., 2018), using a Gaussian radial basis function (RBF) kernel and $\sigma = 1$. Unless stated otherwise, all parameters were left to their default values. Resampling was performed with the `mlr` package (Bischl et al., 2016).

Significance levels for all tests were fixed at $\alpha = 0.05$. For each simulation, we calculated the CPI values, Type I errors, Type II errors, empirical coverage, and t-statistics, where applicable. Results for MSE loss are shown in Fig. 1. Similar plots for MAE, CE, and MMCE loss functions are presented in Figs. S1-S7 of the supplement. Coverage probabilities are shown in Tables S1-S8 of the supplement.

For continuous outcomes, CPI controlled Type I error with all four learners and reached 100% power under all settings, with the exception of the LM on nonlinear data. We observed no difference between the MSE and MAE loss functions.

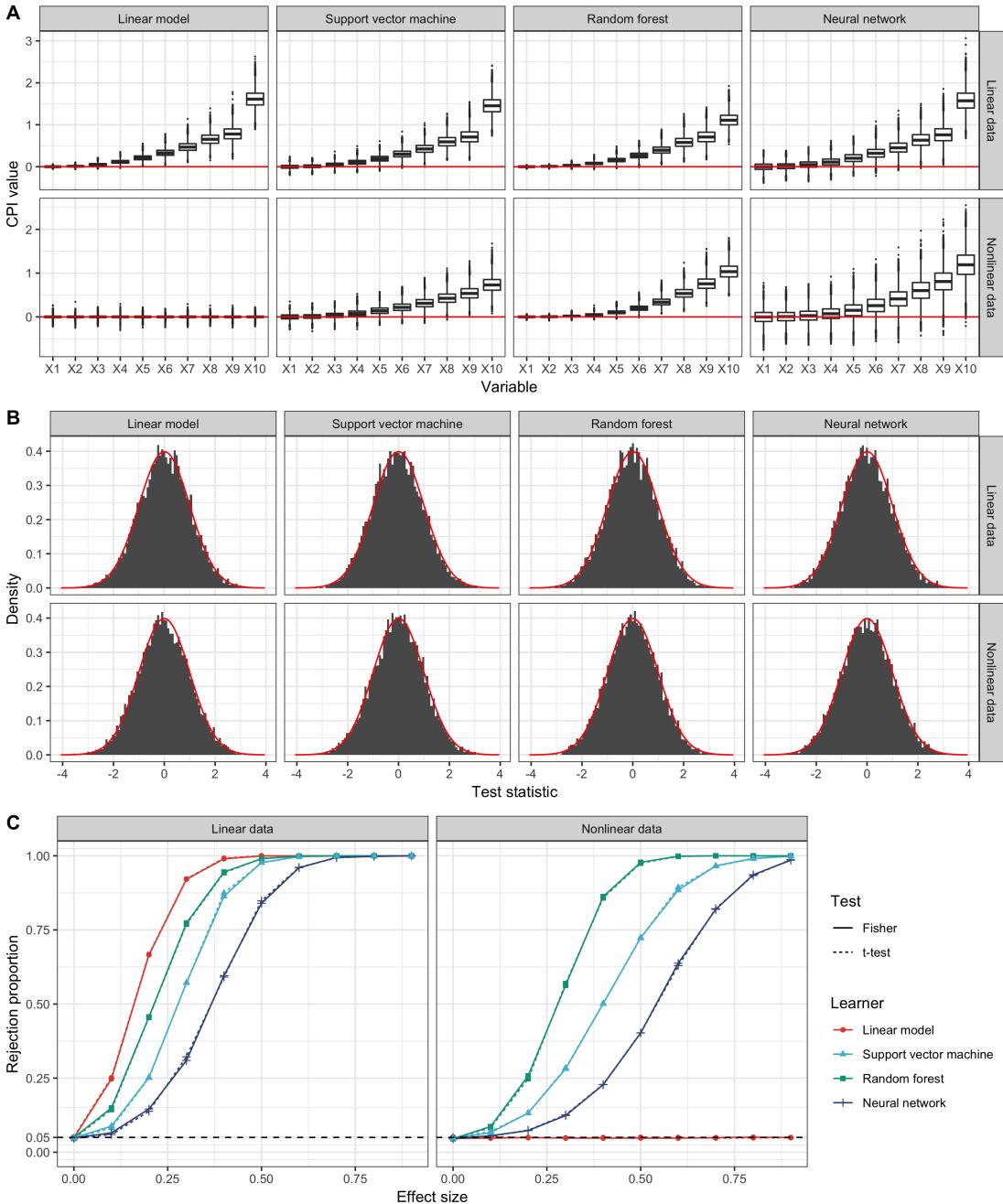We found similar results for categorical outcomes. The CPI controlled Type I error for

16

Figure 1: Simulation results for continuous outcome with MSE loss and correlated predictors. **A**: Boxplots of simulated CPI values of variables $X_1, \ldots, X_{10}$ with increasing effect size. The red line indicates a CPI value of 0, corresponding to a completely uninformative predictor X_j. **B**: Histograms of simulation replications of t-statistics of variables with effect size 0. The distribution of the expected t-statistic under the null hypothesis is shown in red. **C**: Proportion of rejected hypotheses at $\alpha = 0.05$ as a function of effect size. Results at effect size 0 correspond to the Type I error, at effect sizes > 0 to statistical power. The dashed line indicates the nominal level of $\alpha = 0.05$.

17

the MMCE and CE loss functions with all four learners. The LM once again performed poorly on nonlinear data, as expected. The Fisher test had slightly increased power compared to the t-test. Statistical power was generally greater with CE loss than with MMCE loss.

4.1.2 Comparative Performance

We use the same simulation setup to compare the CPI's performance to that of three other global, nonparametric, model-agnostic measures of CI:

- **ANOVA**: Williamson et al. (2017)'s nonparametric ANOVA-inspired VI.
- **LOCO**: Lei et al. (2018)'s leave-one-covariate-out procedure.
- **GCM**: Shah and Peters (forthcoming)'s generalized covariance measure.

Unfortunately, software for Hubbard et al. (2018)'s targeted maximum likelihood VI statistic was still under development at the time of testing, and beta versions generated errors. Candès et al.'s probabilistic knockoff procedure (2018) can be extended to nonparametric models, but requires an algorithm-specific VI measure, which not all learners provide. We consider this method separately in Section 4.1.3. Kernel methods do not work with arbitrary algorithms and were therefore excluded. We restrict this section to the regression setting, as none of the other methods considered here are designed for classification problems.

Training and test sets are of equal size, with $n = \{100, 500, 1000\}$. In each case, we fit LM, RF, ANN, and SVM regressions, as described previously. We estimate the VI of all features on the test set for every model. This procedure was repeated 10,000 times. Results for $n = 1,000$ are plotted in Fig. 2. Similar results for smaller sample sizes are included in the supplement.

All methods have high Type II error rates when fitting an LM to nonlinear data, highlighting the dangers of model misspecification. GCM appears to dominate in the linear setting, but struggles to detect VI in nonlinear simulations. LOCO is somewhat conservative, often falling short of the nominal Type I error rate under the null hypothesis. However, the method fails to control Type I error in the case of an ANN trained on nonlinear data. The
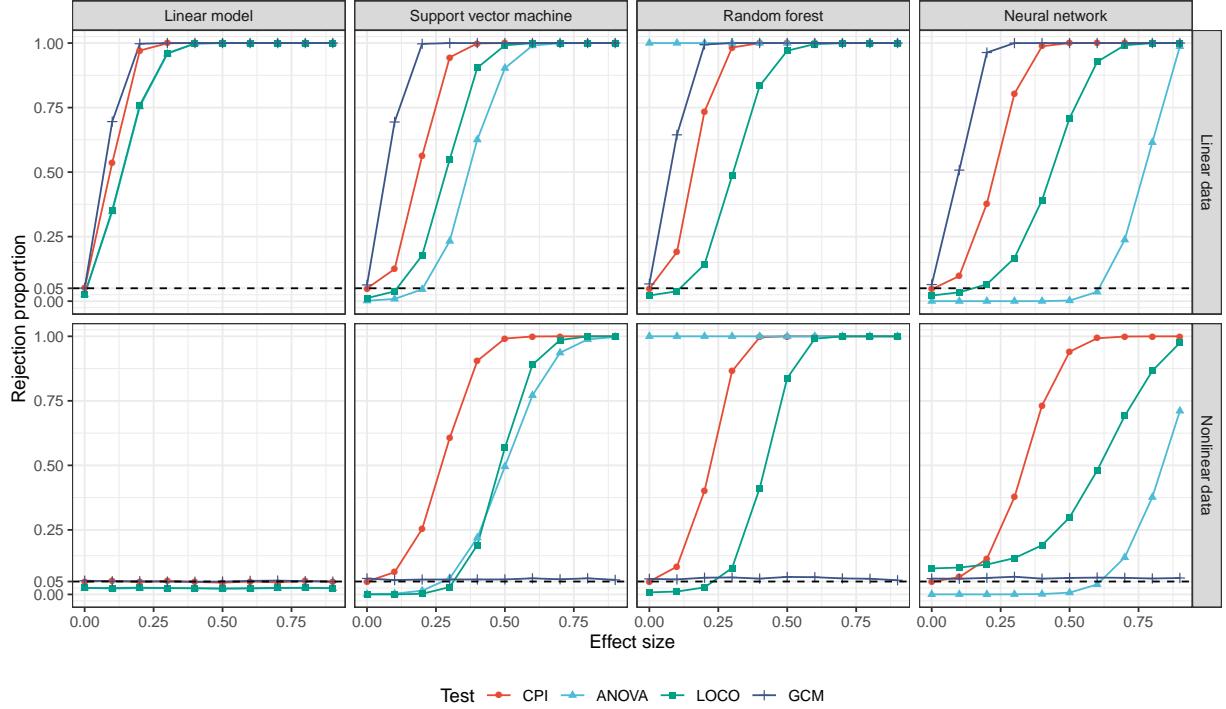
Figure 2: Comparative performance of VI measures across different simulations and algorithms. Plots depict the proportion of rejected hypotheses at $\alpha = 0.05$ as a function of effect size. Results at effect size 0 correspond to Type I error, at effect sizes > 0 to statistical power. The dashed line indicates the nominal level of $\alpha = 0.05$. These results were computed using training and test samples of $n = 1,000$. Similar results were obtained for sample sizes of $n = 500$ and $n = 100$ (see Supplementary Materials).

nonparametric ANOVA generally performs poorly, especially with RF regressions, where we observed Type I error rates of up to 100%.

The CPI outperforms all competitors with nonlinear data, and achieves greater power than ANOVA or LOCO in the linear case. GCM is the only other method to control Type I error under all simulation settings, but it has nearly zero power with nonlinear data.

4.1.3 Knockoff Filter

To compare the performance of the CPI with that of the original knockoff filter, we followed the simulation procedure described in Section 4 of (Candès et al., 2018). A $n = 300 \times p =$

1,000 feature matrix was sampled from a multivariate Gaussian distribution $\mathcal{N}(0, \Sigma)$ with covariance matrix $\Sigma_{ij} = \rho^{|i-j|}$. A continuous outcome Y was calculated as $\mathbf{X}\boldsymbol{\beta} + \epsilon$, where $\epsilon \sim \mathcal{N}(0, 1)$ and the coefficient vector $\boldsymbol{\beta}$ contains just 60 nonzero entries, with random signs and variable effect sizes. We vary ρ with fixed nonzero $|\beta| = 1$, and vary effect size with fixed $\rho = 0$.

We train a series of lasso regressions (Tibshirani, 1996) on the data using the original design matrix and 10-fold cross-validation to calculate the CPI, and the expanded $n \times 2p$ design matrix for the knockoff filter. VI for the latter was estimated using the difference statistic originally proposed by Barber and Candès (2015):

$$W_j = |\hat{\beta}_j| - |\hat{\beta}_{j+p}|$$

where $\hat{\beta}_j$ and $\hat{\beta}_{j+p}$ represent the coefficients associated with a feature and its knockoff, respectively, at some fixed value of the Lagrange multiplier λ. Variables are selected based on the ATT method described in Section 2.3. We tune λ via 10-fold cross-validation, per the default settings of the `glmnet` package (Friedman et al., 2010). Power and FDR are averaged over $10,000$ iterations for each combination of effect size and autocorrelation coefficient.

The CPI is more powerful than the original knockoff filter for all effect sizes at $\rho = 0$, but less powerful for high autocorrelation of $\rho > 0.5$ (see Fig. 3). Both methods generally control the FDR at the target rate of 10%. The only exceptions are under small effect sizes, where the knockoff filter shows slightly inflated errors.

Note that in addition to being a more powerful test under most conditions, the CPI has other important advantages over the ATT. Whereas the latter can only be applied to algorithms with inbuilt feature scoring statistics, the former requires nothing more than a valid loss function. Whereas the ATT struggles to select important variables in low-dimensional settings, the CPI imposes no dimensionality restraints. Finally, the CPI is more informative, insomuch as it provides feature-level p-values and confidence (or credible) intervals.
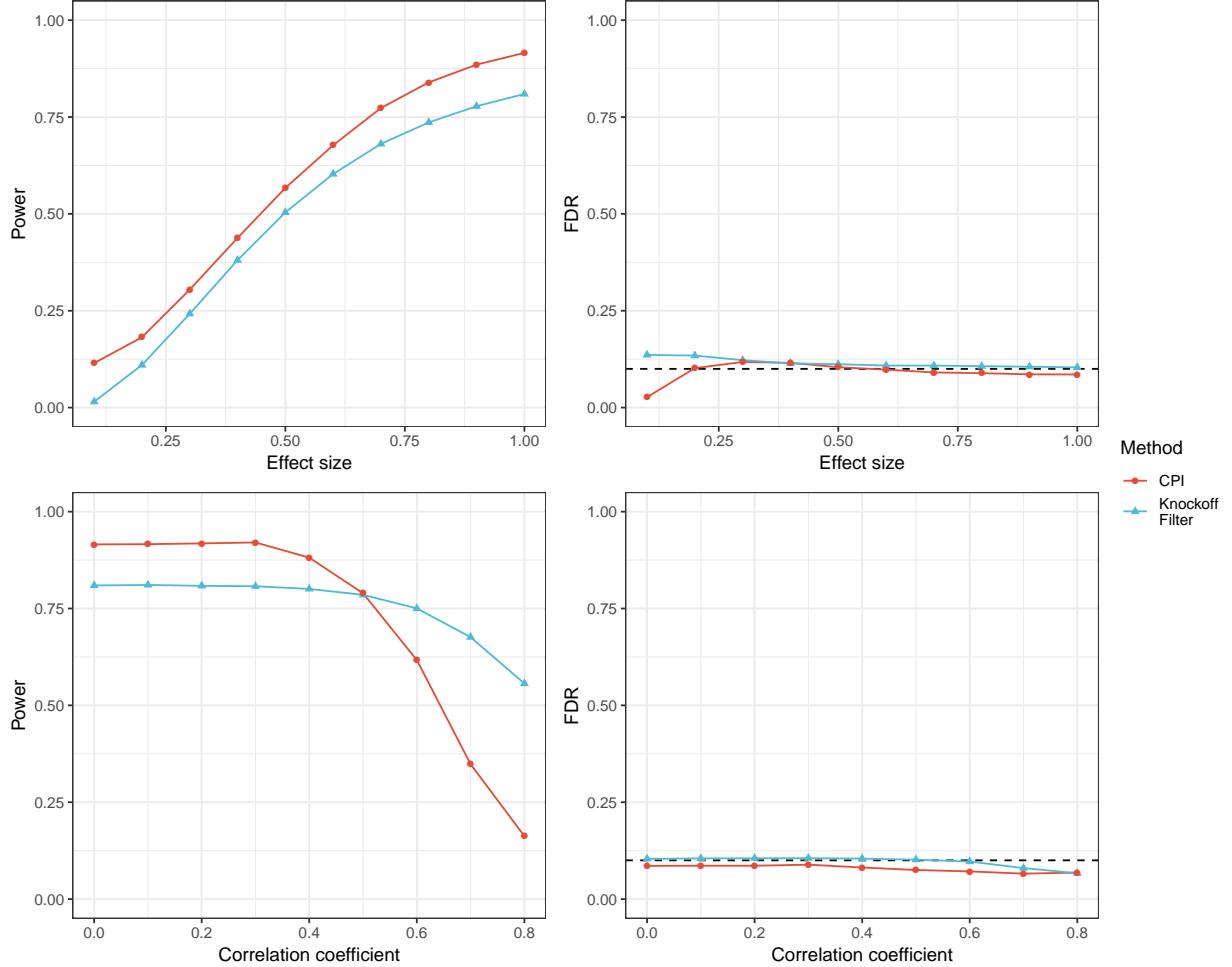
Figure 3: Power and FDR as a function of effect size and autocorrelation for CPI and knockoff filter. Target FDR is 10%. Results are from a lasso regression with $n = 300$ and $p = 1,000$. Each point represents 10,000 replications.

4.2 Real Data

In this section, we apply the CPI to real datasets of low- and high-dimensionality.

4.2.1 Boston Housing

We analyzed the Boston housing data (Harrison and Rubinfeld, 1978), which consists of 506 observations and 14 variables. This benchmark dataset is available in the UCI Machine Learning Repository (Dua and Taniskidou, 2017). The dependent variable is the
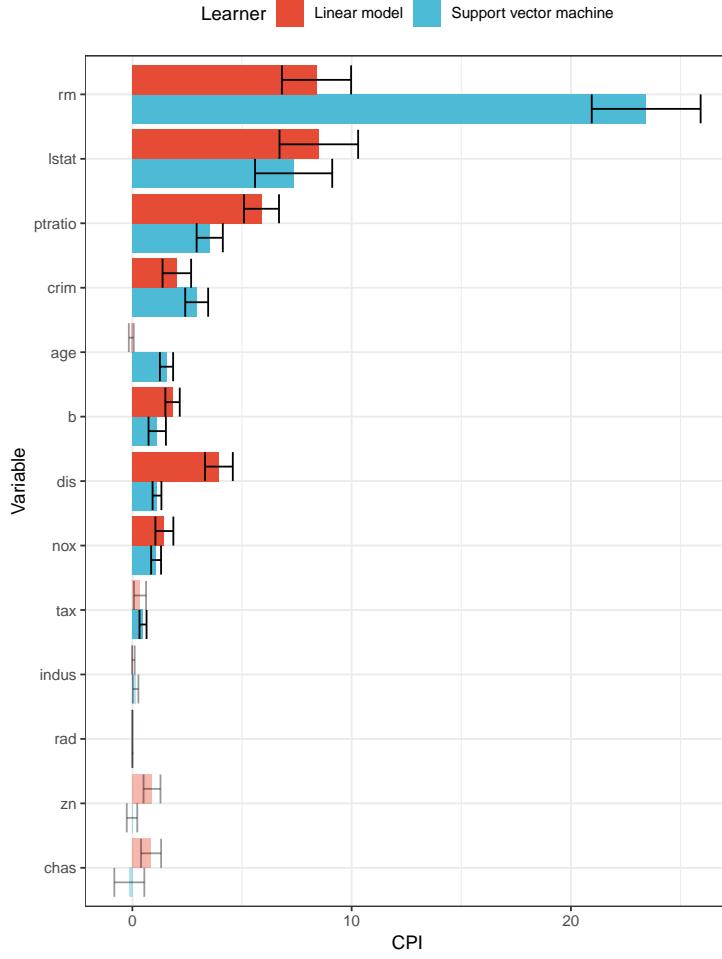
Figure 4: Results of the Boston housing experiment. For each variable in the data set, the CPI value is shown, computed with a linear model and a support vector machine. Whiskers represent standard errors. Non-significant variables at $\alpha = 0.05$ after adjustment for multiple testing are shaded.

median price of owner-occupied houses in census tracts in the Boston metropolitan area in 1970. The independent variables include the average number of rooms, crime rates, and air pollution.

Using LM and SVM regressions, we computed CPI, standard errors, and t-test p-values for each feature, adjusting for multiple testing using Holm's (1979) procedure. We used an RBF kernel for the SVM, measured performance via MSE, and used 5 subsampling iterations to evaluate empirical risk. The results are shown in Fig. 4. We found significant

effects at $\alpha = 0.05$ for the average number of rooms (`rm`), percentage of lower status of the population (`lstat`), pupil-teacher ratio (`ptratio`), and several other variables with both LM and SVM, which is in line with previous analyses (Friedman and Popescu, 2008; Williamson et al., 2017). Interestingly, the SVM assigned a higher CPI value to several variables compared to the LM. For example, the proportion of owner-occupied units built prior to 1940 (`age`) significantly increased the predictive performance of the SVM but had approximately zero impact on the LM. The reason for this difference might be a nonlinear interaction between `rm` and `age`, which was also observed by Friedman and Popescu (2008).

4.2.2 Breast Cancer

We examined gene expression profiles of human breast cancer samples downloaded from GEO series GSE3165. Only the 94 arrays of platform GPL887 (Agilent Human 1A Microarray V2) were included. These data were originally analyzed by Herschkowitz et al. (2007) and later studied by Lim et al. (2009). We follow their preprocessing pipeline, leaving 13,064 genes. All samples were taken from tumor tissue and classified into one of six molecular subtypes: basal-like, luminal A, luminal B, Her2, normal-like, and claudin-low.

Basal-like breast cancer (BLBC) is an especially aggressive form of the disease, and BLBC patients generally have a poor prognosis. Following Wu and Smyth (2012), we define a binary response vector to indicate whether or not samples are BLBC. Gene sets were downloaded from the curated C2 collection of the MSigDB and tested for their association with this dichotomous outcome.

We trained an RF classifier with 10,000 trees to predict BLBC based on microarray data. Second-order knockoffs were sampled using an approximate semidefinite program with block-diagonal covariance matrices of maximum dimension $4,000 \times 4,000$. We test the CPI for each of the 2,609 gene sets in the C2 collection for which at least 25 genes were present in the expression matrix. Models were evaluated using the CE loss function on out-of-bag samples.

We calculate p-values for each CPI via the t-test and corresponding q-values using the Benjamini-Hochberg procedure (Benjamini and Hochberg, 1995). We identify 660 signifi-
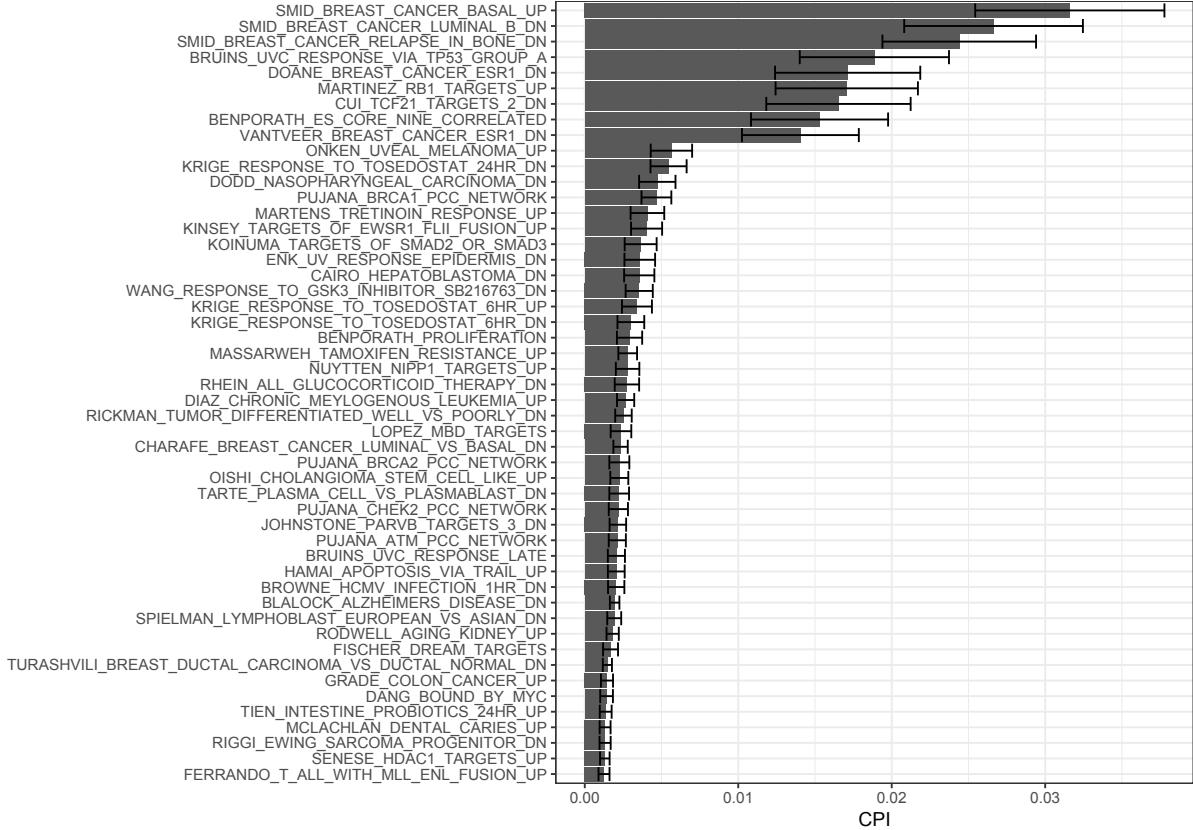
Figure 5: Results for the top 50 gene sets. For each gene set, the CPI value is shown, computed with a random forest. Whiskers represent standard errors.

cantly enriched gene sets at $q \leq 0.05$, including 24 of 73 explicitly breast cancer derived gene sets and 6 of 13 gene sets indicative of basal signatures. Almost all top results are from cancer studies or other biologically relevant research (see Fig. 5). These include 4 sets of BRCA1 targets, genetic mutations known to be associated with BLBC (Turner and Reis-Filho, 2006), and 4 sets of ESR1 targets, which are known markers for the luminal A subtype (Sørlie et al., 2003).

By comparison, popular pathway enrichment tests like GSEA (Subramanian et al., 2005) and CAMERA (Wu and Smyth, 2012) respectively identify 137 and 74 differentially enriched pathways in this dataset at 5% FDR. Our results are especially notable given that those methods rely on marginal associations between gene expression and clinical outcomes, whereas the CPI is a conditional test with a more restrictive null hypothesis,

and should theoretically have less power to detect enrichment when features within a gene set are correlated with others outside it. Despite collinearity between genes, the CPI still identifies a large number of biologically meaningful gene sets differentiating BLBC tumors from other breast cancer subtypes.

5   Discussion

Shah and Peters (forthcoming) have demonstrated that no CI test can be uniformly valid against arbitrary alternatives, a sort of no-free-lunch (NFL) theorem for CI. Bates et al. (2019) prove a similar NFL theorem for constructing knockoff variables, showing that no algorithm can efficiently compute nontrivial knockoffs for arbitrary input distributions. The original NFL theorem for optimization is well-known (Wolpert and Macready, 1997). Together, these results delimit the scope of the CPI. Our method is completely general, in the sense that it works with any well-chosen combination of supervised learner, loss function, and knockoff sampler. However, it is simultaneously constrained by these choices. The CPI will not in general control Type I error or have any power against the null when knockoffs are poorly constructed or models are misspecified.

In our experiments, we employed a variety of risk estimators, including cross-validation, subsampling, out-of-bag estimates, and the holdout method. Results did not depend on these choices, suggesting that analysts may use whichever is most efficient for the problem at hand.

Computational bottlenecks can complicate the use of our procedure for high-dimensional datasets. It took approximately 49 hours to generate second-order knockoffs for the gene expression matrix described in Section 4.2.2. However, as noted in Section 2.3, knockoff sampling is an active area of research, and we expect future advances to speed up the procedure considerably.

6   Conclusion

We propose the conditional predictive impact (CPI), a maximally general test of conditional independence. It works for regression and classification problems using any combination of knockoff sampler, supervised learning algorithm, and loss function. It imposes no parametric or sparsity constraints, and can be efficiently computed on data with many observations and features. Our inference procedures are fast and powerful, able to simultaneously control Type I error and achieve nominal coverage probability. We have shown that our approach is consistent and unbiased under minimal assumptions. Empirical results demonstrate that our method performs favorably against a number of alternatives for a range of supervised learners and data generating processes.

We envision several avenues for future research in this area. Localized versions of the CPI algorithm could be used to detect the conditional importance of features on particular predictions. Model-specific methods could be implemented to speed up the procedure. We are currently working on applications for causal discovery and inference, an especially promising direction for this approach.

Funding

References

Bach, S., Binder, A., Montavon, G., Klauschen, F., Müller, K. R., and Samek, W. (2015), "On pixel-wise explanations for non-linear classifier decisions by layer-wise relevance propagation," *PLoS ONE*, 10, 1–46.

Barber, R. F., and Candès, E. J. (2015), "Controlling the false discovery rate via knockoffs," *Ann. Statist.*, 43, 2055–2085.

Bates, S., Cands, E., Janson, L., and Wang, W. (2019), "Metropolized knockoff sampling," Preprint arXiv:1903.00434.

Benjamini, Y., and Hochberg, Y. (1995), "Controlling the false discovery rate: a practical and powerful approach to multiple testing," *J. Royal Stat. Soc. Ser. B. Methodol.*, 57, 289–300.

Benjamini, Y., and Yekutieli, D. (2001), "The control of the false discovery rate in multiple testing under dependency," *Ann. Statist.*, 29, 1165–1188.

Berrett, T. B., Wang, Y., Barber, R. F., and Samworth, R. J. (2019), "The conditional permutation test for independence while controlling for confounders," *J. Royal Stat. Soc. Ser. B. Methodol.*

Bischl, B., Lang, M., Kotthoff, L., Schiffner, J., Richter, J., Studerus, E., Casalicchio, G., and Jones, Z. M. (2016), "mlr: Machine learning in R," *J. Mach. Learn. Res.*, 17, 1–5.

Breiman, L. (2001), "Random forests," *Mach. Learn.*, 45, 1–33.

Candès, E., Fan, Y., Janson, L., and Lv, J. (2018), "Panning for gold: model-X' knockoffs for high dimensional controlled variable selection," *J. Royal Stat. Soc. Ser. B. Methodol.*, 80, 551–577.

Datta, A., Sen, S., and Zick, Y. (2016), "Algorithmic transparency via quantitative input influence: Theory and experiments with learning systems," *2016 IEEE Symposium on Security and Privacy*, 598–617.

Doran, G., Muandet, K., Zhang, K., and Schölkopf, B. (2014), "A permutation-based kernel conditional independence test," in *Proceedings of the Thirtieth Conference on Uncertainty in Artificial Intelligence*, Arlington, Virginia, United States, pp. 132–141.

Dua, D., and Taniskidou, K. (2017), *UCI Machine Learning Repository*, Irvine, CA: University of California, School of Information and Computer Science.

Feng, J., Williamson, B., Simon, N., and Carone, M. (2018), "Nonparametric variable importance using an augmented neural network with multi-task learning," in *Proceedings of the 35th International Conference on Machine Learning*, Stockholm, Sweden, vol. 80 of *Proceedings of Machine Learning Research*, pp. 1496–1505.

Fisher, A., Rudin, C., and Dominici, F. (2018), "All models are wrong but many are useful:

variable importance for black-box, proprietary, or misspecified prediction models, using model class reliance," Preprint arXiv:1801.01489v4.

Fisher, R. A. (1935), *The Design of Experiments*, London: Oliver & Boyd.

Friedman, J. H., Hastie, T., and Tibshirani, R. (2010), "Regularization paths for generalized linear models via coordinate descent," *J. Stat. Softw.*, 33.

Friedman, J. H., and Popescu, B. E. (2008), "Predictive learning via rule ensembles," *Ann. Appl. Stat.*, 2, 916–954.

Fukumizu, K., Gretton, A., Sun, X., and Schölkopf, B. (2008), "Kernel measures of conditional dependence," in *Advances in Neural Information Processing Systems 20*, pp. 489–496.

Gevrey, M., Dimopoulos, I., and Lek, S. (2003), "Review and comparison of methods to study the contribution of variables in artificial neural network models," *Ecol. Model.*, 160, 249–264.

Gregorutti, B., Michel, B., and Saint-Pierre, P. (2015), "Grouped variable importance with random forests and application to multiple functional data analysis," *Comput. Stat. Data Anal.*, 90, 15–35.

Grömping, U. (2007), "Estimators of relative importance in linear regression based on variance decomposition," *Am. Stat.*, 61, 139–147.

Guyon, I., and Elisseeff, A. (2003), "An introduction to variable and feature selection." *J. Mach. Learn. Res.*, 3, 1157–1182.

Harrison, D., and Rubinfeld, D. L. (1978), "Hedonic housing prices and the demand for clean air," *J. Environ. Econ. Manag.*, 5, 81–102.

Herschkowitz, J. I., Simin, K., Weigman, V. J., Mikaelian, I., Usary, J., Hu, Z., Rasmussen, K. E., Jones, L. P., Assefnia, S., Chandrasekharan, S., Backlund, M. G., Yin, Y., Khramtsov, A. I., Bastein, R., Quackenbush, J., Glazer, R. I., Brown, P. H., Green, J. E., Kopelovich, L., Furth, P. A., Palazzo, J. P., Olopade, O. I., Bernard, P. S., Churchill, G. A., Van Dyke, T., and Perou, C. M. (2007), "Identification of conserved gene expression features between murine mammary carcinoma models and human breast tumors," *Genome Biol.*, 8, R76.

Holm, S. (1979), "A simple sequentially rejective multiple test procedure," *Scand. J. Stat.*, 6, 65–70.

Hubbard, A. E., Kennedy, C. J., and van der Laan, M. J. (2018), "Data-adaptive target parameters," in *Targeted Learning in Data Science*, New York: Springer, chap. 9, pp. 125–142.

Jordon, J., Yoon, J., and van der Schaar, M. (2019), "KnockoffGAN: Generating knockoffs for feature selection using generative adversarial networks," in *International Conference on Learning Representations*, New Orleans, USA.

Kalisch, M., Mächler, M., Colombo, D., Maathuis, M. H., and Bühlmann, P. (2012), "Causal inference using graphical models with the R package pcalg," *J. Stat. Softw.*, 47, 1–26.

Koller, D., and Friedman, N. (2009), *Probabilistic Graphical Models: Principles and Techniques*, Cambridge, MA: MIT Press.

Korb, K. B., and Nicholson, A. E. (2009), *Bayesian Artificial Intelligence*, Boca Raton, FL: Chapman and Hall/CRC, 2nd ed.

Kruschke, J. K. (2013), "Bayesian estimation supersedes the *t*-test," *J. Exp. Psychol. Gen.*, 142, 573.

Kuhn, M., and Johnson, K. (2019), *Feature Engineering and Selection: A Practical Approach for Predictive Models*, Boca Raton, FL: Chapman and Hall/CRC.

Kursa, M. B., and Rudnicki, W. R. (2010), "Feature selection with the boruta package," *J. Stat. Softw.*, 36.

Lei, J., G'Sell, M., Rinaldo, A., Tibshirani, R. J., and Wasserman, L. (2018), "Distribution-free predictive inference for regression," *J. Am. Stat. Assoc.*, 113, 1094–1111.

Lim, E., Vaillant, F., Wu, D., Forrest, N. C., Pal, B., Hart, A. H., Asselin-Labat, M.-L., Gyorki, D. E., Ward, T., Partanen, A., Feleppa, F., Huschtscha, L. I., Thorne, H. J., KConFab, Fox, S. B., Yan, M., French, J. D., Brown, M. A., Smyth, G. K., Visvader, J. E., and Lindeman, G. J. (2009), "Aberrant luminal progenitors as the candidate target population for basal tumor development in BRCA1 mutation carriers," *Nat. Med.*, 15, 907.

Lindeman, R. H., Merenda, P. F., and Gold, R. Z. (1980), *Introduction to Bivariate and Multivariate Analysis*, Glenview, IL: Longman.

Lundberg, S. M., and Lee, S.-I. (2017), in *Advances in Neural Information Processing Systems 30*, eds. Guyon, I., Luxburg, U. V., Bengio, S., Wallach, H., Fergus, R., Vishwanathan, S., and Garnett, R., Curran Associates, Inc., pp. 4765–4774.

Maathuis, M. H., Kalisch, M., and Bühlmann, P. (2009), "Estimating high-dimensional intervention effects from observational data," *Ann. Statist.*, 37, 3133–3164.

Meinshausen, N.— (2010), "Stability selection," *J. Royal Stat. Soc. Ser. B. Methodol.*, 72, 417–473.

Mentch, L., and Hooker, G. (2016), "Quantifying uncertainty in random forests via confidence intervals and hypothesis tests," *J. Mach. Learn. Res.*, 17, 841–881.

Meyer, D., Dimitriadou, E., Hornik, K., Weingessel, A., and Leisch, F. (2018), *e1071: Misc Functions of the Department of Statistics, Probability Theory Group, TU Wien*, R package version 1.7-0.

Nicodemus, K. K., Malley, J. D., Strobl, C., and Ziegler, A. (2010), "The behaviour of random forest permutation-based variable importance measures under predictor correlation," *BMC Bioinform.*, 11, 110.

Patterson, E., and Sesia, M. (2018), *knockoff: The Knockoff Filter for Controlled Variable Selection*, R package version 0.3.2.

Pearl, J. (1988), *Probabilistic Reasoning in Intelligent Systems: Networks of Plausible Inference*, San Mateo, CA: Morgan Kaufmann.

Phipson, B., and Smyth, G. (2010), "Permutation P-values should never be zero: calculating exact P-values when permutations are randomly drawn," *Stat. Appl. Genet. Mol. Biol.*, 9.

R Core Team (2018), "R: A Language and Environment for Statistical Computing," Vienna, Austria.

Ramsey, J. D. (2014), "A scalable conditional independence test for nonlinear, non-gaussian data," Preprint arXiv:1401.5031v2.

Ribeiro, M. T., Singh, S., and Guestrin, C. (2016), ""Why Should I Trust You?": Ex-

plaining the Predictions of Any Classifier," in *Proceedings of the 22nd ACM SIGKDD International Conference on Knowledge Discovery and Data Mining*, New York, NY, USA: ACM, KDD '16, pp. 1135–1144.

Rinaldo, A., Wasserman, L., and G'Sell, M. (2019), "Bootstrapping and sample splitting for high-dimensional, assumption-lean inference," *Ann. Statist.*, 47, 3438–3469.

Romano, Y., Sesia, M., and Cands, E. J. (2018), "Deep knockoffs," Preprint arXiv:1811.06687.

Rouder, J. N., Speckman, P. L., Sun, D., Morey, R. D., and Iverson, G. (2009), "Bayesian *t*-tests for accepting and rejecting the null hypothesis," *Psychon. Bull. Rev.*, 16, 225–237.

Sauer, N. (1972), "On the density of families of sets," *J. Comb. Theory Ser. A*, 13, 145–147.

Scutari, M. (2010), "Learning Bayesian networks with the bnlearn R package," *J. Stat. Softw.*, 35, 1–22.

Scutari, M., and Denis, J.-B. (2014), *Bayesian Networks: With Examples in R*, Boca Raton, FL: Chapman and Hall/CRC.

Sesia, M., Sabatti, C., and Cands, E. J. (2018), "Gene hunting with hidden Markov model knockoffs," *Biometrika*, 106, 1–18.

Shah, R., and Peters, J. (forthcoming), "The hardness of conditional independence testing and the generalised covariance measure," *Ann. Statist.*, preprint arXiv:1804.07203v2.

Shelah, S. (1972), "A combinatorial problem: stability and orders for models and theories in infinitariy languages," *Pac. J. Math.*, 41, 247–261.

Shrikumar, A., Greenside, P., and Kundaje, A. (2017), "Learning Important Features Through Propagating Activation Differences," in *Proceedings of the 34th International Conference on Machine Learning - Volume 70*, JMLR.org, ICML'17, pp. 3145–3153.

Sørlie, T., Tibshirani, R., Parker, J., Hastie, T., Marron, J. S., Nobel, A., Deng, S., Johnsen, H., Pesich, R., Geisler, S., Demeter, J., Perou, C. M., Lønning, P. E., Brown, P. O., Børresen-Dale, A.-L., and Botstein, D. (2003), "Repeated observation of breast tumor subtypes in independent gene expression data sets," *Proc. Natl. Acad. Sci.*, 100, 8418–8423.

Spirtes, P., Glymour, C. N., and Scheines, R. (2000), *Causation, Prediction, and Search*, Cambridge, MA: MIT Press, 2nd ed.

Storey, J. D. (2002), "A direct approach to false discovery rates," *J. Royal Stat. Soc. Ser. B. Methodol.*, 64, 479–498.

Strobl, C., Boulesteix, A.-L., Kneib, T., Augustin, T., and Zeileis, A. (2008), "Conditional variable importance for random forests," *BMC Bioinform.*, 9, 307.

Strobl, E. V., Kun, Z., and Shyam, V. (2018), "Approximate Kernel-Based Conditional Independence Tests for Fast Non-Parametric Causal Discovery," *Journal of Causal Inference*, 7.

Subramanian, A., Tamayo, P., Mootha, V. K., Mukherjee, S., Ebert, B. L., Gillette, M. A., Paulovich, A., Pomeroy, S. L., Golub, T. R., Lander, E. S., and Mesirov, J. P. (2005), "Gene set enrichment analysis: A knowledge-based approach for interpreting genome-wide expression profiles," *Proc. Natl. Acad. Sci.*, 102, 15545–15550.

Tansey, W., Veitch, V., Zhang, H., Rabadan, R., and Blei, D. M. (2018), "The hold-out randomization test: principled and easy black box feature selection," Preprint arXiv:1811.00645.

Tibshirani, R. (1996), "Regression shrinkage and selection via the Lasso," *J. Royal Stat. Soc. Ser. B. Methodol.*, 58, 267–288.

Turner, N. C., and Reis-Filho, J. S. (2006), "Basal-like breast cancer and the BRCA1 phenotype," *Oncogene*, 25, 5846.

van der Laan, M. J. (2006), "Statistical inference for variable importance," *Int. J. Biostat.*, 2.

van der Laan, M. J., and Rose, S. (eds.) (2018), *Targeted Learning in Data Science*, New York: Springer.

Vapnik, V., and Chervonenkis, A. (1971), "On the uniform convergence of relative frequencies to their probabilities," *Theory Probab. Appl.*, 16, 264–280.

Venables, W. N., and Ripley, B. D. (2002), *Modern Applied Statistics with S*, New York: Springer, 4th ed.

Verma, T., and Pearl, J. (1991), "Equivalence and synthesis of causal models," in *Proceed-*

ings of the Sixth Annual Conference on Uncertainty in Artificial Intelligence, New York, NY, USA, pp. 255–270.

Wachter, S., Mittelstadt, B., and Russell, C. (2018), "Counterfactual explanations without opening the black box: automated decisions and the GDPR," *Harvard Journal of Law and Technology*, 31, 841–887.

Wetzels, R., Raaijmakers, J. G., Jakab, E., and Wagenmakers, E.-J. (2009), "How to quantify support for and against the null hypothesis: A flexible WinBUGS implementation of a default Bayesian t-test," *Psychon. Bull. Rev.*, 16, 752–760.

Williamson, B., Gilbert, P., Simon, N., and Carone, M. (2017), "Nonparametric variable importance assessment using machine learning techniques," Preprint UW Biostatistics Working Paper 422.

Wolpert, D. H., and Macready, W. G. (1997), "No free lunch theorems for optimization," *IEEE Trans. Evol. Comput.*, 1, 67–82.

Wright, M. N., and Ziegler, A. (2017), "ranger: A fast implementation of random forests for high dimensional data in C++ and R," *J. Stat. Softw.*, 77.

Wu, D., and Smyth, G. K. (2012), "Camera: a competitive gene set test accounting for inter-gene correlation," *Nucleic Acids Res.*, 40, e133.

Zhang, K., Peters, J., Janzing, D., and Schölkopf, B. (2011), "Kernel-based Conditional Independence Test and Application in Causal Discovery," in *Proceedings of the Twenty-Seventh Conference on Uncertainty in Artificial Intelligence*, Arlington, Virginia, United States: AUAI Press, UAI'11, pp. 804–813.

Supplementary Material for "Testing Conditional Independence in Supervised Learning Algorithms"

December 17, 2019

Learner	Linear data		Non-linear data	
	t-Test	Fisher	t-Test	Fisher
Linear model	0.9514	0.9485	0.9533	0.9479
Support vector machine	0.9516	0.9550	0.9528	0.9527
Random forest	0.9505	0.9537	0.9546	0.9529
Neural network	0.9518	0.9533	0.9548	0.9501

Table S1: Empirical coverage probabilities of 95% confidence intervals in the simulation study, calculated from 10,000 simulation replicates; continuous outcome with MSE loss function; correlated predictors.

Learner	Linear data		Non-linear data	
	t-Test	Fisher	t-Test	Fisher
Linear model	0.9523	0.9496	0.9517	0.9531
Support vector machine	0.9517	0.9491	0.9521	0.9539
Random forest	0.9500	0.9516	0.9498	0.9495
Neural network	0.9557	0.9544	0.9521	0.9532

Table S2: Empirical coverage probabilities of 95% confidence intervals in the simulation study, calculated from 10,000 simulation replicates; continuous outcome with MAE loss function; correlated predictors.

Learner	Linear data		Non-linear data	
	t-Test	Fisher	t-Test	Fisher
Linear model	0.9494	0.9484	0.9549	0.9514
Support vector machine	0.9514	0.9544	0.9518	0.9542
Random forest	0.9533	0.9544	0.9503	0.9537
Neural network	0.9537	0.9525	0.9493	0.9538

Table S3: Empirical coverage probabilities of 95% confidence intervals in the simulation study, calculated from 10,000 simulation replicates; continuous outcome with MSE loss function; uncorrelated predictors.

Learner	Linear data		Non-linear data	
	t-Test	Fisher	t-Test	Fisher
Linear model	0.9522	0.9486	0.9525	0.9502
Support vector machine	0.9511	0.9515	0.9513	0.9534
Random forest	0.9518	0.9511	0.9509	0.9517
Neural network	0.9506	0.9470	0.9508	0.9538

Table S4: Empirical coverage probabilities of 95% confidence intervals in the simulation study, calculated from 10,000 simulation replicates; continuous outcome with MAE loss function; uncorrelated predictors.

Learner	Linear data		Non-linear data	
	t-Test	Fisher	t-Test	Fisher
Logistic regression	0.7405	0.9576	0.9029	0.9493
Support vector machine	0.9034	0.9525	0.9260	0.9503
Random forest	0.8585	0.9473	0.9080	0.9454
Neural network	0.9303	0.9529	0.9357	0.9519

Table S5: Empirical coverage probabilities of 95% confidence intervals in the simulation study, calculated from 10,000 simulation replicates; classification outcome with MMCE loss function; correlated predictors.

Learner	Linear data		Non-linear data	
	t-Test	Fisher	t-Test	Fisher
Logistic regression	0.9511	0.9516	0.9510	0.9511
Support vector machine	0.9514	0.9520	0.9534	0.9495
Random forest	0.9503	0.9499	0.9521	0.9503
Neural network	0.9493	0.9522	0.9517	0.9518

Table S6: Empirical coverage probabilities of 95% confidence intervals in the simulation study, calculated from 10,000 simulation replicates; classification outcome with CE loss function; correlated predictors.

Learner	Linear data		Non-linear data	
	t-Test	Fisher	t-Test	Fisher
Logistic regression	0.7651	0.9525	0.8968	0.9523
Support vector machine	0.9164	0.9503	0.9262	0.9532
Random forest	0.9023	0.9439	0.9110	0.9507
Neural network	0.9345	0.9504	0.9369	0.9514

Table S7: Empirical coverage probabilities of 95% confidence intervals in the simulation study, calculated from 10,000 simulation replicates; classification outcome with MMCE loss function; uncorrelated predictors.

Learner	Linear data		Non-linear data	
	t-Test	Fisher	t-Test	Fisher
Logistic regression	0.9510	0.9480	0.9487	0.9469
Support vector machine	0.9488	0.9492	0.9527	0.9493
Random forest	0.9532	0.9524	0.9499	0.9516
Neural network	0.9522	0.9523	0.9494	0.9522

Table S8: Empirical coverage probabilities of 95% confidence intervals in the simulation study, calculated from 10,000 simulation replicates; classification outcome with CE loss function; uncorrelated predictors.
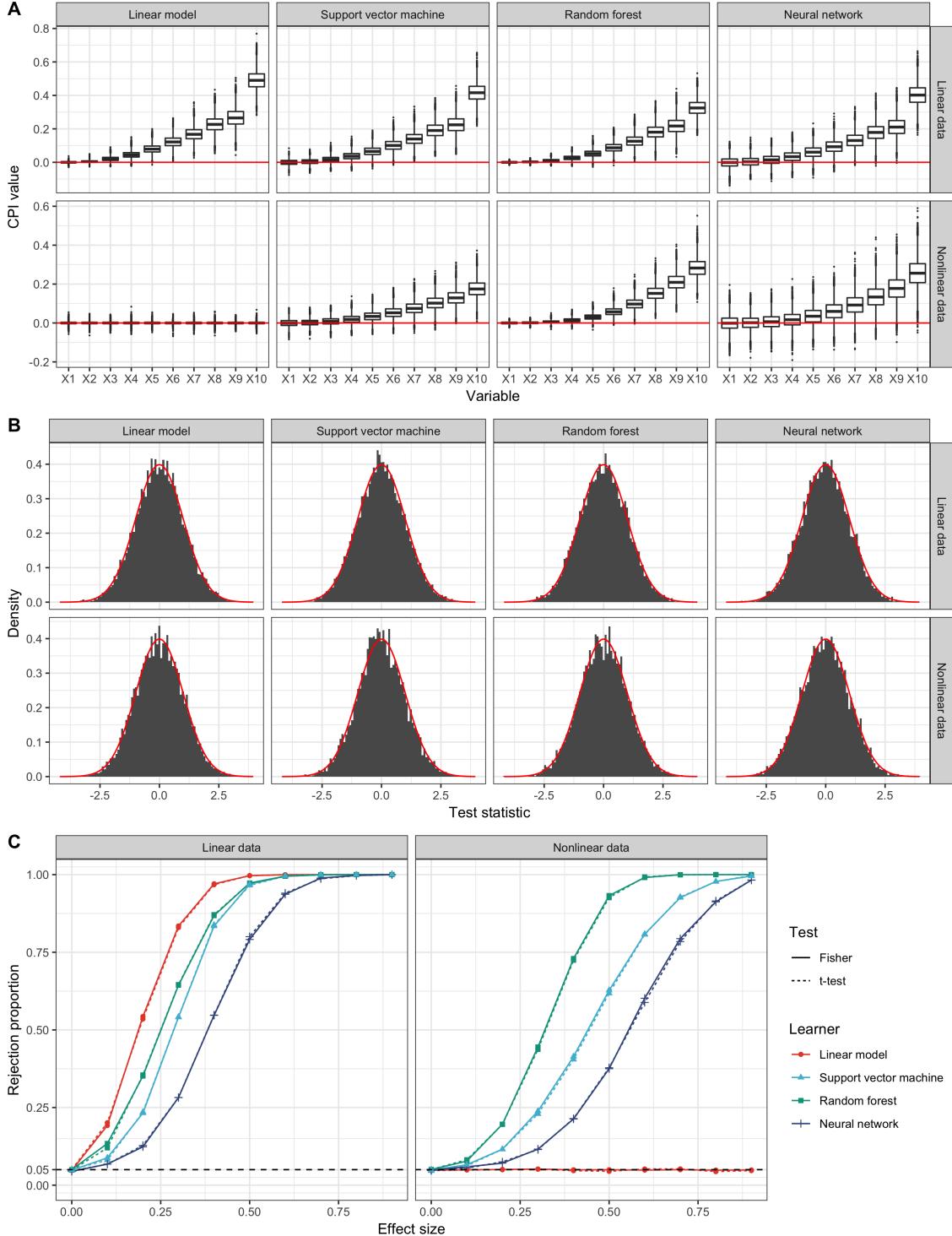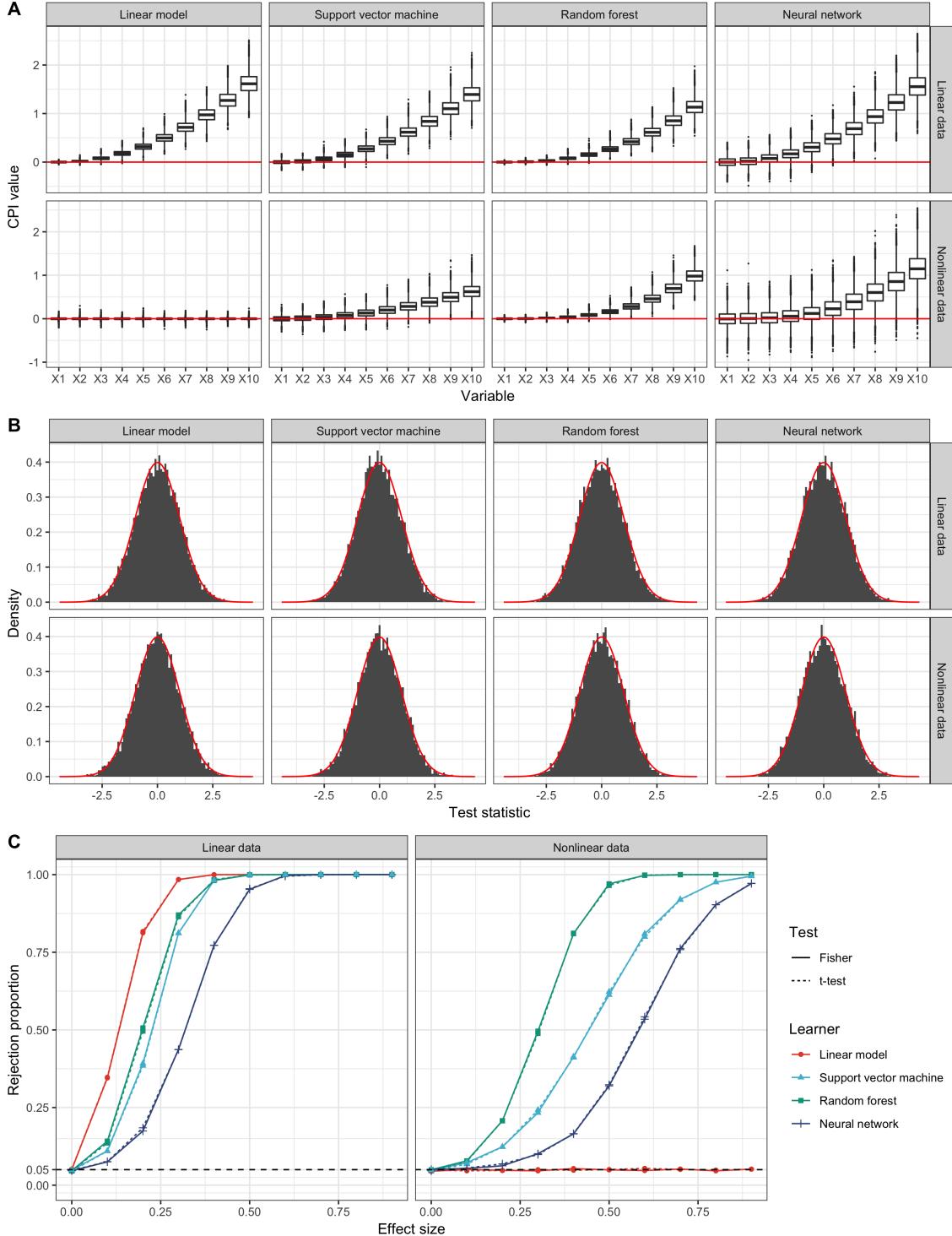
Figure S1: Simulation results for continuous outcome with MAE loss function and correlated predictors. **A**: Boxplots of simulation replications of CPI values of variables $X_1, \ldots, X_{10}$ with increasing effect size. The red line indicates a CPI value of 0, corresponding to no estimated association between the variable X_j and the outcome Y. **B**: Histograms of simulation replications of t-statistics of variables with effect size 0. The distribution of the expected t-statistic under the null hypothesis is shown in red. **C**: Average proportion of rejected hypotheses at $\alpha = 0.05$. Results at effect size 0 correspond to the type I error, at effect sizes > 0 to statistical power. The dashed line indicates the nominal level of $\alpha = 0.05$. The panels correspond to the simulation scenario, the colors and symbols to the learning algorithms and the line types to the inference procedure.
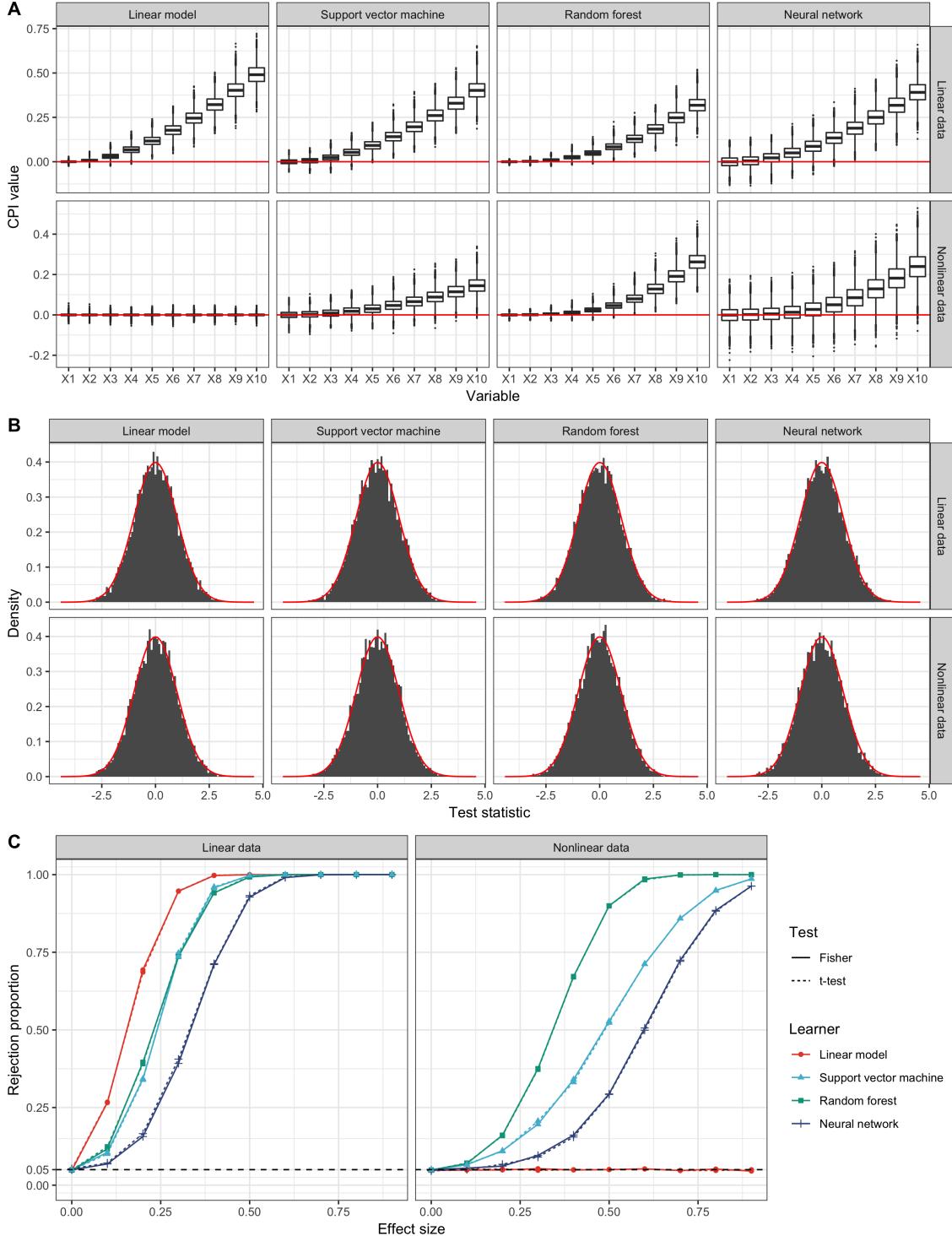
Figure S2: Simulation results for continuous outcome with MSE loss function and uncorrelated predictors. **A**: Boxplots of simulation replications of CPI values of variables $X_1, \ldots, X_{10}$ with increasing effect size. The red line indicates a CPI value of 0, corresponding to no estimated association between the variable X_j and the outcome Y. **B**: Histograms of simulation replications of t-statistics of variables with effect size 0. The distribution of the expected t-statistic under the null hypothesis is shown in red. **C**: Average proportion of rejected hypotheses at $\alpha = 0.05$. Results at effect size 0 correspond to the type I error, at effect sizes > 0 to statistical power. The dashed line indicates the nominal level of $\alpha = 0.05$. The panels correspond to the simulation scenario, the colors and symbols to the learning algorithms and the line types to the inference procedure.
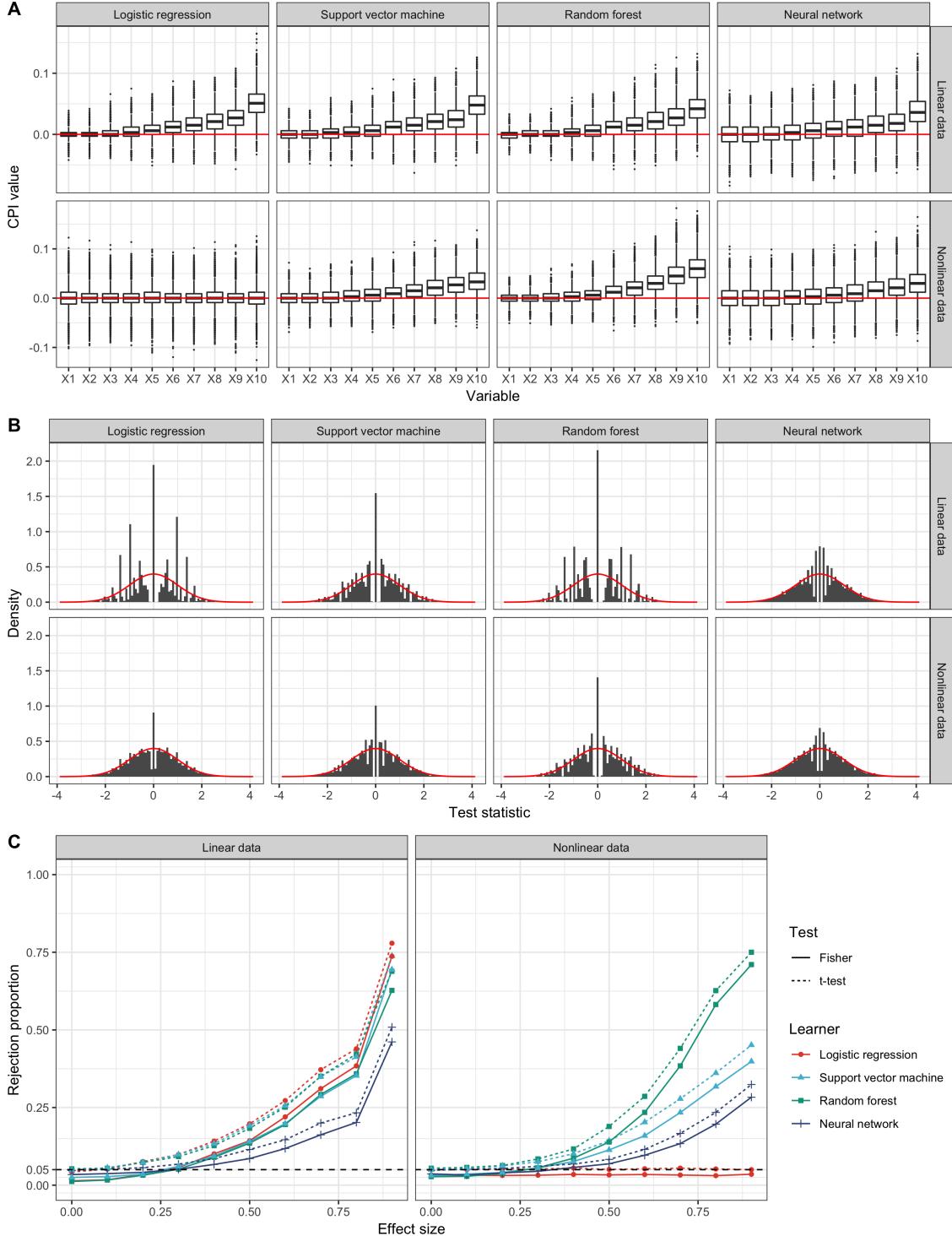
4

Figure S3: Simulation results for continuous outcome with MAE loss function and uncorrelated predictors. **A**: Boxplots of simulation replications of CPI values of variables $X_1, \ldots, X_{10}$ with increasing effect size. The red line indicates a CPI value of 0, corresponding to no estimated association between the variable X_j and the outcome Y. **B**: Histograms of simulation replications of t-statistics of variables with effect size 0. The distribution of the expected t-statistic under the null hypothesis is shown in red. **C**: Average proportion of rejected hypotheses at $\alpha = 0.05$. Results at effect size 0 correspond to the type I error, at effect sizes > 0 to statistical power. The dashed line indicates the nominal level of $\alpha = 0.05$. The panels correspond to the simulation scenario, the colors and symbols to the learning algorithms and the line types to the inference procedure.
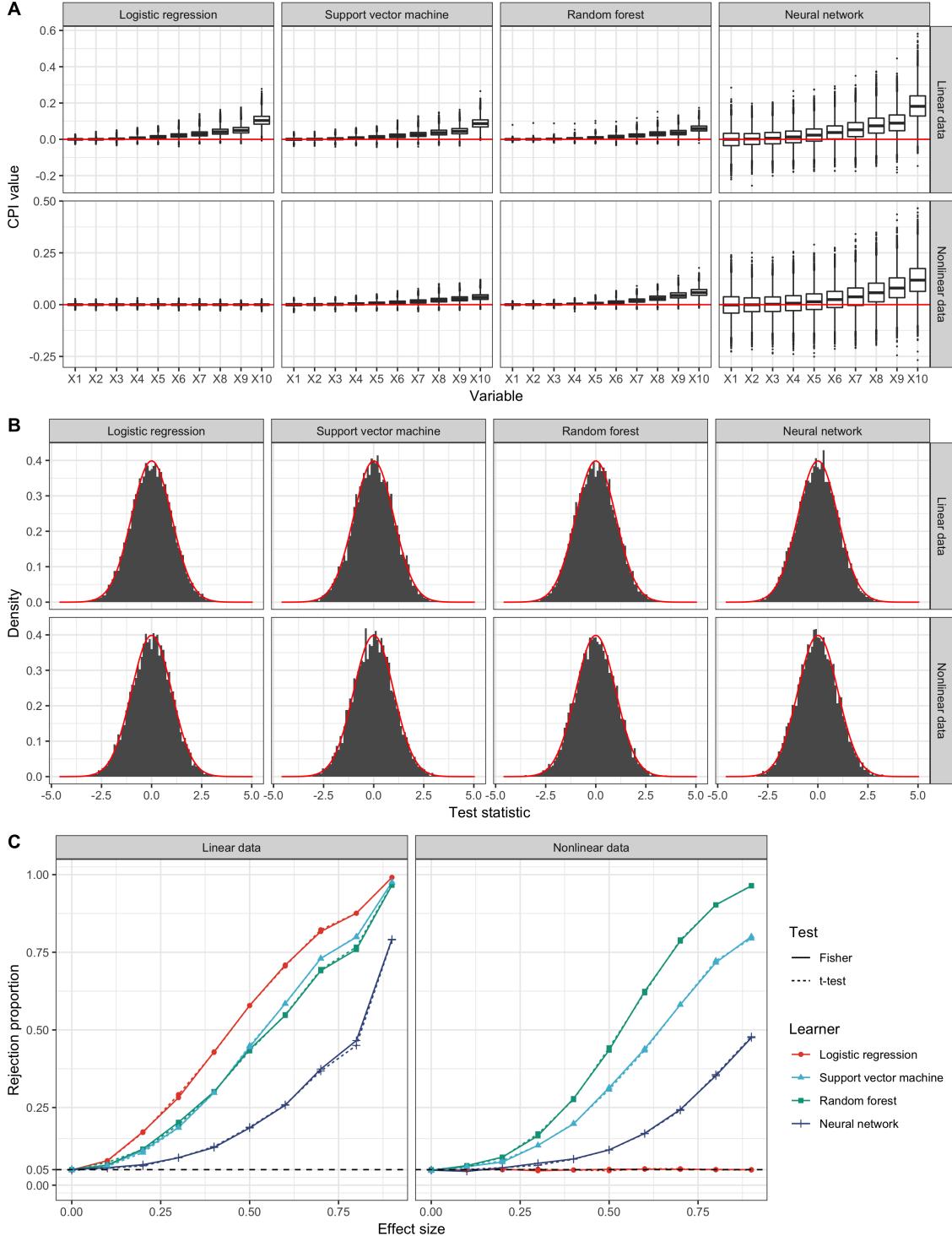
5

Figure S4: Simulation results for classification outcome with MMCE loss function and correlated predictors. **A**: Boxplots of simulation replications of CPI values of variables $X_1, \ldots, X_{10}$ with increasing effect size. The red line indicates a CPI value of 0, corresponding to no estimated association between the variable X_j and the outcome Y. **B**: Histograms of simulation replications of t-statistics of variables with effect size 0. The distribution of the expected t-statistic under the null hypothesis is shown in red. **C**: Average proportion of rejected hypotheses at $\alpha = 0.05$. Results at effect size 0 correspond to the type I error, at effect sizes > 0 to statistical power. The dashed line indicates the nominal level of $\alpha = 0.05$. The panels correspond to the simulation scenario, the colors and symbols to the learning algorithms and the line types to the inference procedure.
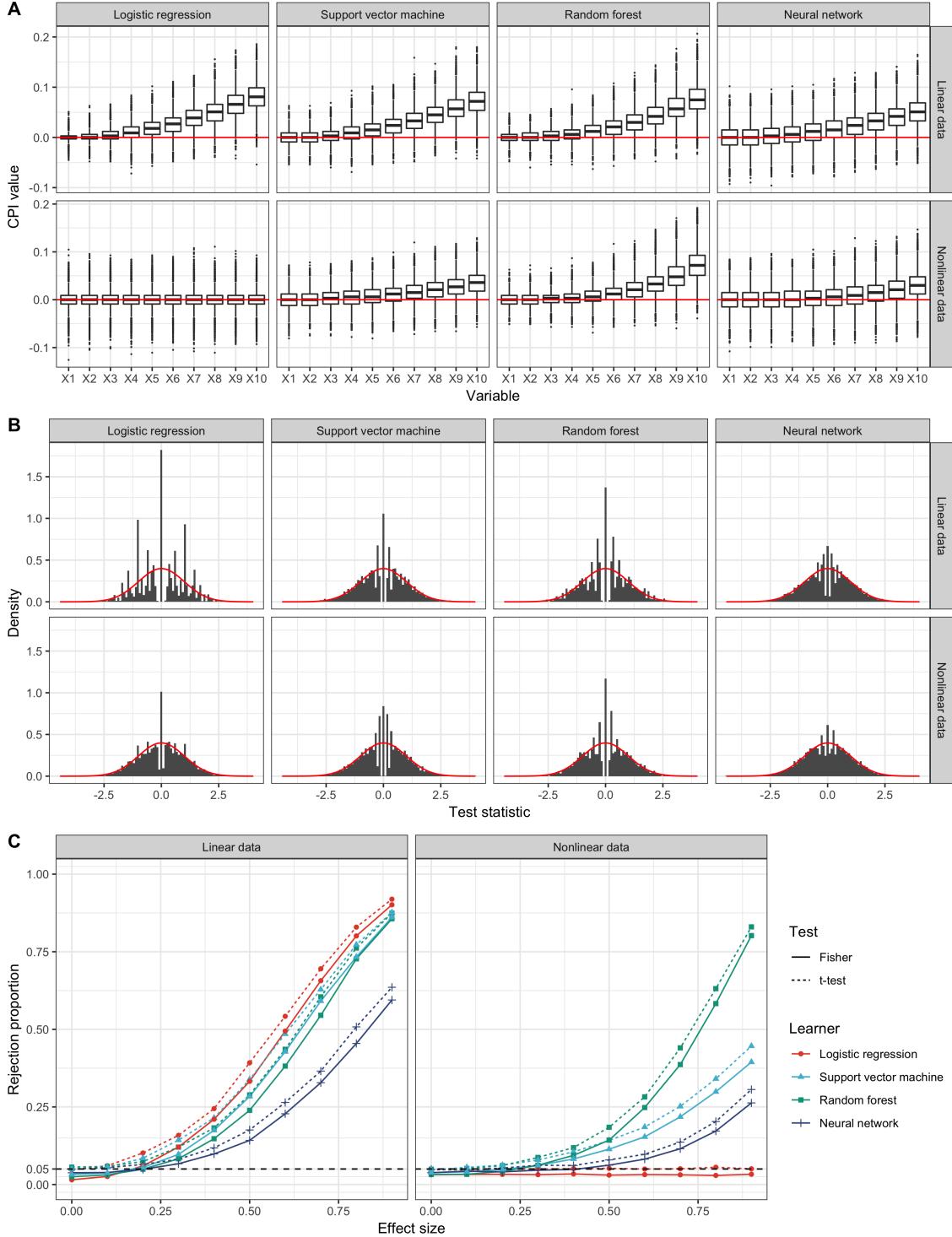
Figure S5: Simulation results for classification outcome with CE loss function and correlated predictors. **A**: Boxplots of simulation replications of CPI values of variables $X_1, \ldots, X_{10}$ with increasing effect size. The red line indicates a CPI value of 0, corresponding to no estimated association between the variable X_j and the outcome Y. **B**: Histograms of simulation replications of t-statistics of variables with effect size 0. The distribution of the expected t-statistic under the null hypothesis is shown in red. **C**: Average proportion of rejected hypotheses at $\alpha = 0.05$. Results at effect size 0 correspond to the type I error, at effect sizes > 0 to statistical power. The dashed line indicates the nominal level of $\alpha = 0.05$. The panels correspond to the simulation scenario, the colors and symbols to the learning algorithms and the line types to the inference procedure.
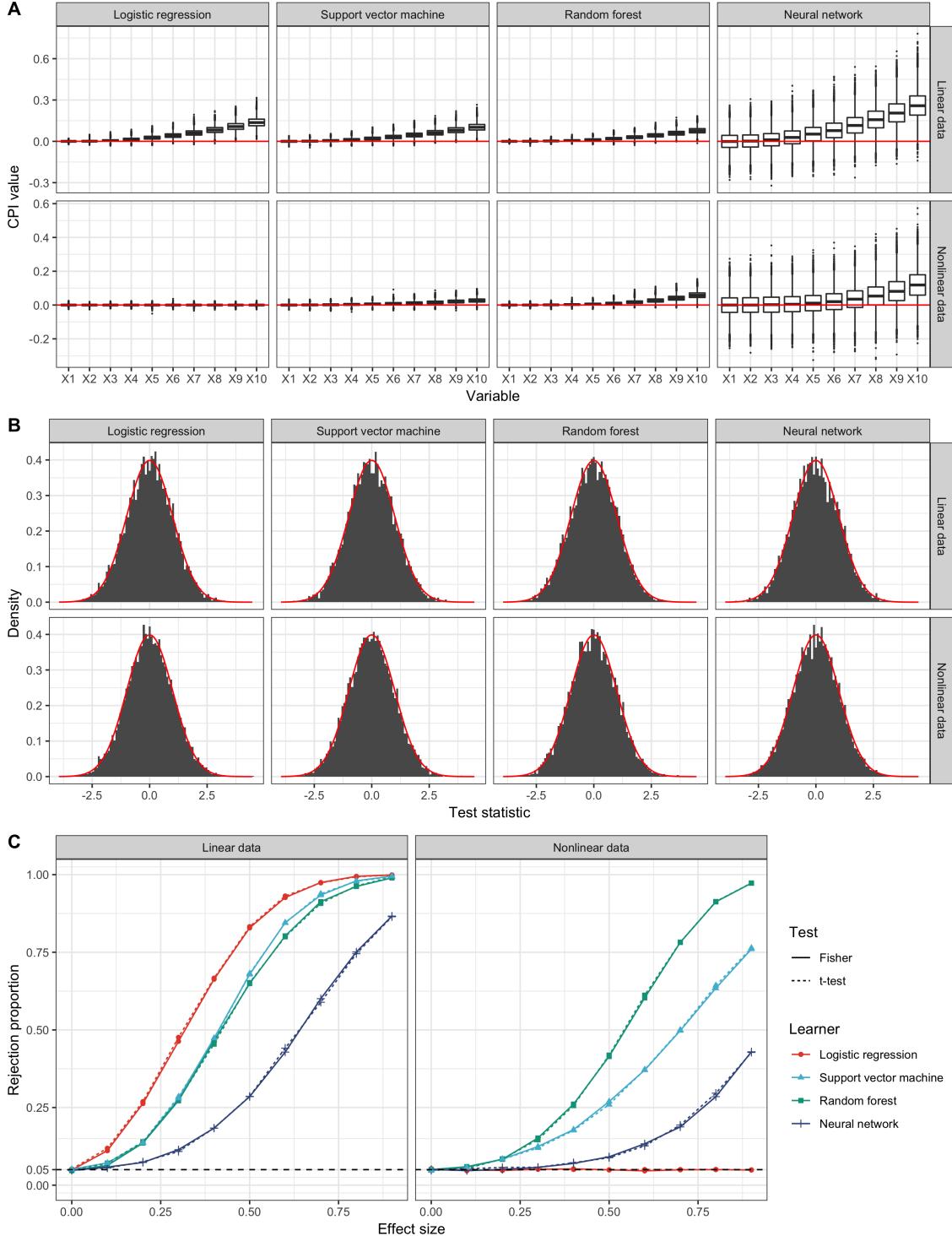
7

Figure S6: Simulation results for classification outcome with MMCE loss function and uncorrelated predictors. **A**: Boxplots of simulation replications of CPI values of variables $X_1, \ldots, X_{10}$ with increasing effect size. The red line indicates a CPI value of 0, corresponding to no estimated association between the variable X_j and the outcome Y. **B**: Histograms of simulation replications of t-statistics of variables with effect size 0. The distribution of the expected t-statistic under the null hypothesis is shown in red. **C**: Average proportion of rejected hypotheses at $\alpha = 0.05$. Results at effect size 0 correspond to the type I error, at effect sizes > 0 to statistical power. The dashed line indicates the nominal level of $\alpha = 0.05$. The panels correspond to the simulation scenario, the colors and symbols to the learning algorithms and the line types to the inference procedure.

8

Figure S7: Simulation results for classification outcome with CE loss function and uncorrelated predictors. **A**: Boxplots of simulation replications of CPI values of variables $X_1, \ldots, X_{10}$ with increasing effect size. The red line indicates a CPI value of 0, corresponding to no estimated association between the variable X_j and the outcome Y. **B**: Histograms of simulation replications of t-statistics of variables with effect size 0. The distribution of the expected t-statistic under the null hypothesis is shown in red. **C**: Average proportion of rejected hypotheses at $\alpha = 0.05$. Results at effect size 0 correspond to the type I error, at effect sizes > 0 to statistical power. The dashed line indicates the nominal level of $\alpha = 0.05$. The panels correspond to the simulation scenario, the colors and symbols to the learning algorithms and the line types to the inference procedure.
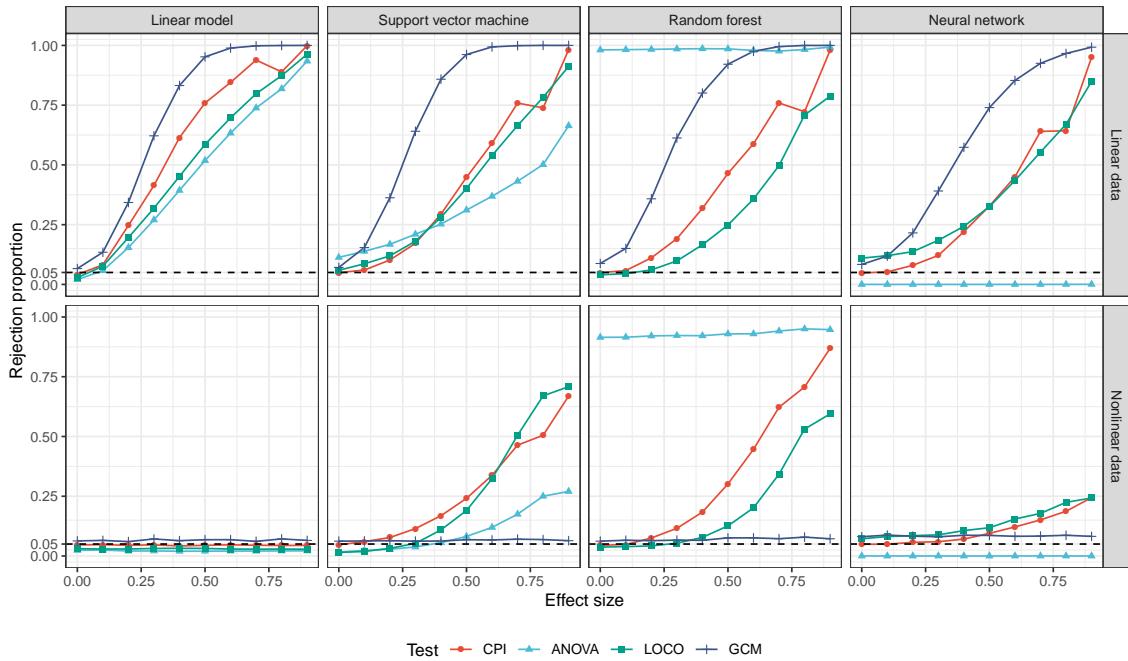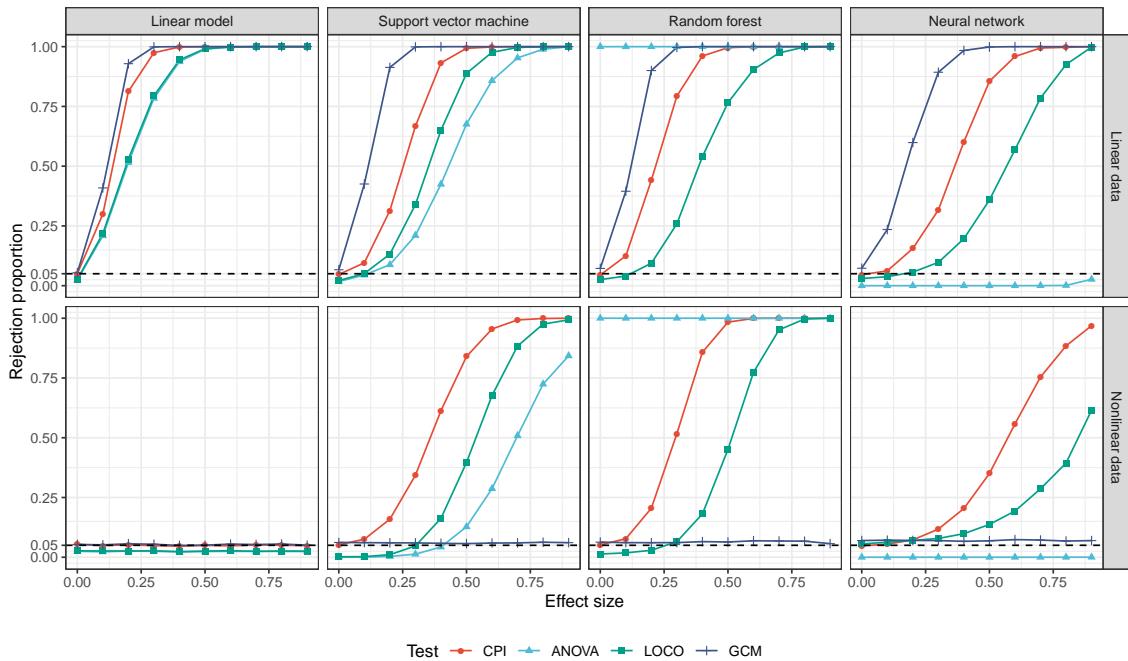
Figure S8: Comparative performance of VI measures across different simulations and algorithms, computed with a training and test sample of $n = 100$ and correlated predictors. Plots depict the proportion of rejected hypotheses at $\alpha = 0.05$ as a function of effect size. Results at effect size 0 correspond to Type I error, at effect sizes > 0 to statistical power. The dashed line indicates the nominal level of $\alpha = 0.05$.
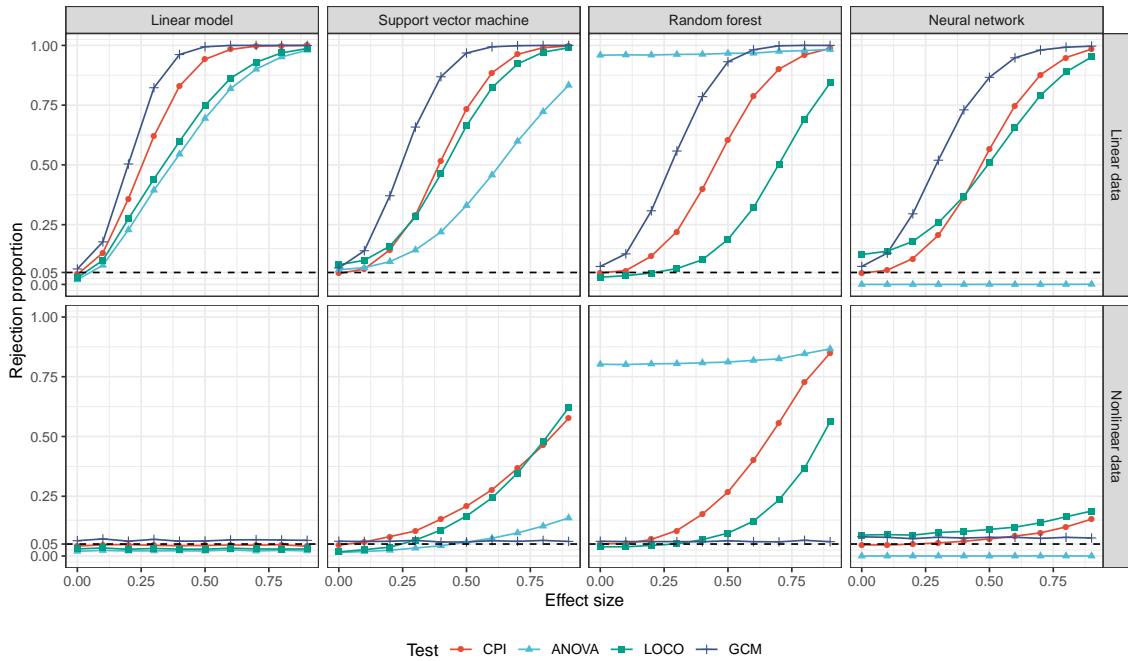

Figure S9: Comparative performance of VI measures across different simulations and algorithms, computed with a training and test sample of $n = 500$ and correlated predictors. Plots depict the proportion of rejected hypotheses at $\alpha = 0.05$ as a function of effect size. Results at effect size 0 correspond to Type I error, at effect sizes > 0 to statistical power. The dashed line indicates the nominal level of $\alpha = 0.05$.

Figure S10: Comparative performance of VI measures across different simulations and algorithms, computed with a training and test sample of $n = 100$ and uncorrelated predictors. Plots depict the proportion of rejected hypotheses at $\alpha = 0.05$ as a function of effect size. Results at effect size 0 correspond to Type I error, at effect sizes > 0 to statistical power. The dashed line indicates the nominal level of $\alpha = 0.05$.
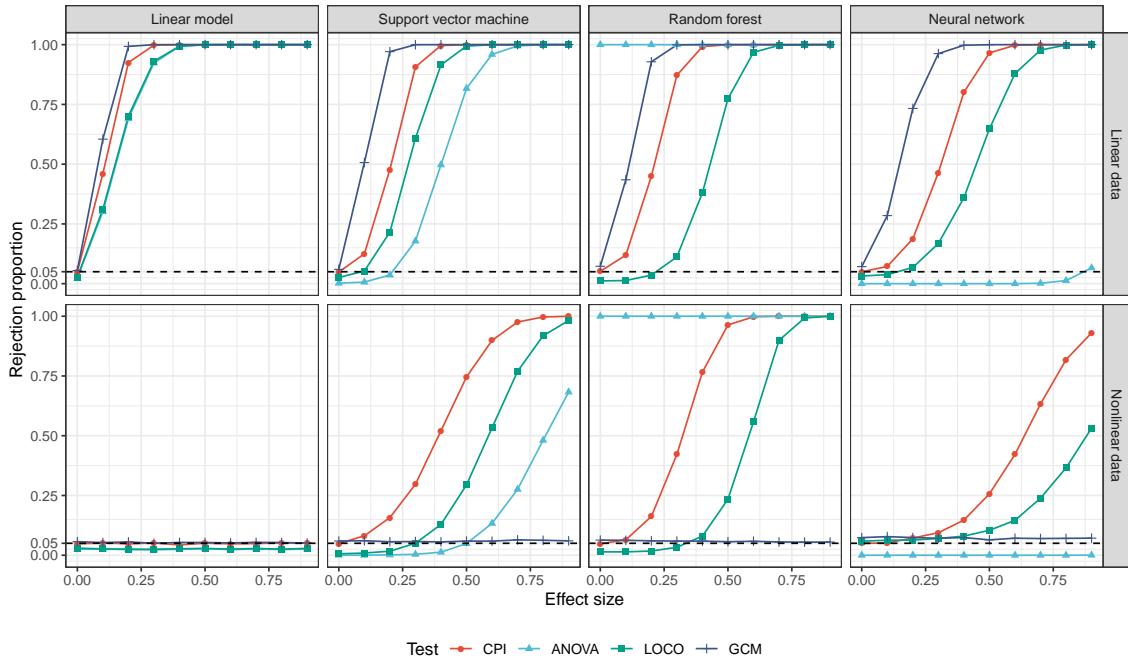

Figure S11: Comparative performance of VI measures across different simulations and algorithms, computed with a training and test sample of $n = 500$ and uncorrelated predictors. Plots depict the proportion of rejected hypotheses at $\alpha = 0.05$ as a function of effect size. Results at effect size 0 correspond to Type I error, at effect sizes > 0 to statistical power. The dashed line indicates the nominal level of $\alpha = 0.05$.
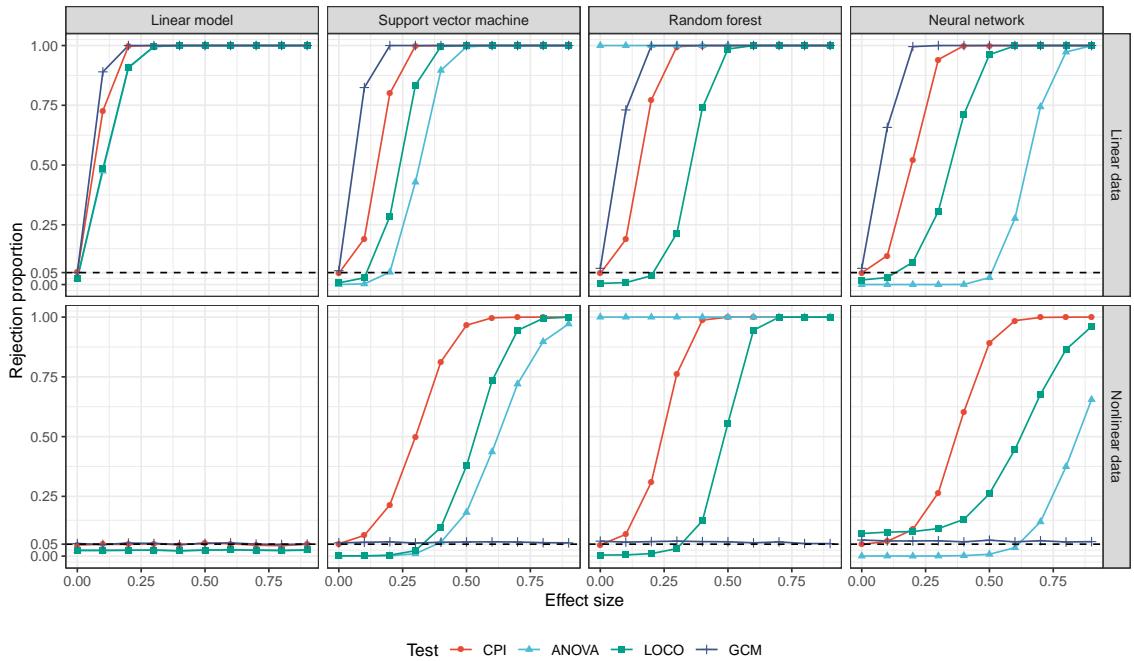
Figure S12: Comparative performance of VI measures across different simulations and algorithms, computed with a training and test sample of $n = 1000$ and uncorrelated predictors. Plots depict the proportion of rejected hypotheses at $\alpha = 0.05$ as a function of effect size. Results at effect size 0 correspond to Type I error, at effect sizes > 0 to statistical power. The dashed line indicates the nominal level of $\alpha = 0.05$.